

# Future global water scarcity partially moderated by vegetation responses to rising CO<sub>2</sub>

Jessica Stacey<sup>1,2</sup>, Richard A. Betts<sup>1,2</sup>, Andrew Hartley<sup>2</sup>, Lina Mercado<sup>3,4</sup>, Nicola Gedney<sup>2</sup>

<sup>1</sup>Global Systems Institute, University of Exeter, Exeter, EX4 4QJ, UK

5 <sup>2</sup>Met Office Hadley Centre, Exeter, EX1 3PB, UK

<sup>3</sup>Environment, Science & Economy, University of Exeter, Exeter, EX4 4QJ, UK

<sup>4</sup>UK Centre for Ecology and Hydrology, Wallingford, EX10 8BB, UK

*Correspondence to:* Jessica Stacey (jessica.stacey@metoffice.gov.uk)

**Abstract.** Most studies of future water scarcity rely on hydrological models that often neglect the effects of plant physiological responses to rising CO<sub>2</sub> on the water cycle, such as reduced stomatal opening, which can decrease transpiration and enhance water availability over large scales. To evaluate how plant physiological and structural responses to rising CO<sub>2</sub> and subsequent climate change affect water scarcity in typical impact studies, we replicate their experimental design by driving an offline land surface model with Earth system model output. Under a high-emission climate scenario, our simulations suggest that combined plant responses increase water supply and partially alleviate water scarcity for most regions, largely due to CO<sub>2</sub>-induced stomatal closure. However, CO<sub>2</sub>- and climate-induced vegetation changes do exacerbate water scarcity in some places, particularly arid regions. For the period 2076–2095, incorporating all plant responses to CO<sub>2</sub> and climate change reduces global median Water Scarcity Index (WSI) by approximately 12%. Furthermore, across 291 river basins, 138 basins show lower median WSI (by 10-70%), representing 80% of the global population, while 11 basins show higher WSI (by 10-60%), representing 0.2% of the population. These results indicate that CO<sub>2</sub>-induced plant responses may partially moderate future water scarcity, although worsening water scarcity is still projected in many regions, including highly populated areas. Overall, these findings suggest that accounting for plant stomatal and structural responses to rising CO<sub>2</sub> warrants consideration in water scarcity assessments.

**Short summary.** Plants typically transpire less with rising atmospheric carbon dioxide, leaving more water in the ground for human use, but many future water scarcity assessments ignore this effect. We use a land surface model to examine how plant responses to carbon dioxide and climate change affect future water scarcity. Our results suggest that including these plant responses increases overall water availability for most people, highlighting the importance of their inclusion in future water scarcity studies.

## 1 Introduction

30 Throughout this manuscript, we use the following terminology.

- **Stomatal (physiological) response:** Changes in plant water-use efficiency due to adjustments in stomatal aperture.

- **Vegetation structural response:** Changes in vegetation structure, including leaf area and canopy coverage.
- **Combined (or total) vegetation response:** The combined response of stomatal and vegetation structural responses.

35 Accurately predicting future water scarcity, where water demand exceeds available supply, remains a complex but vital task  
for informing long-term adaptation strategies (Caretta et al., 2022). Current impact studies on future water scarcity are typically  
based on output from hydrological models driven by climate model outputs (e.g., Dolan et al., 2021; Gosling and Arnell, 2016;  
Greve et al., 2018; Haddeland et al., 2014). While hydrological models are powerful tools for understanding, managing, and  
planning water resources, they often lack a representation of vegetation response to rising levels of CO<sub>2</sub> and climate change.  
40 In this study, we investigate the influence that these vegetation responses have on water scarcity projections.

Water scarcity is a complex and multifaceted issue influenced by water availability, demand, and quality. Nearly half of the  
global population already faces severe water scarcity at some point each year, and as both population and consumption rates  
rise, water demand is escalating (Caretta et al. 2022; Ripple et al., 2017). Water availability, crucial for meeting this rising  
45 demand, depends on the balance between land precipitation and evapotranspiration, both of which are strongly affected by  
human activities, including climate change. Climate change is altering precipitation patterns and near-surface meteorological  
conditions, driving more frequent hydrological extremes and higher evaporative demand (Seneviratne et al., 2021). Human  
interventions—such as groundwater over-abstraction, dam construction, and water diversion—further disrupt water supply,  
while pollution threatens the availability of clean water. Many future water scarcity projections rely on standalone hydrological  
50 models driven by global climate model outputs (e.g., Dolan et al., 2021; Gosling and Arnell, 2016; Greve et al., 2018;  
Haddeland et al., 2014; Schewe et al., 2013). These studies generally project worsening water scarcity in many regions due to  
both climate change and rising demand, with the most affected areas including parts of northern and southern Africa, south  
and southeast Asia, Australia, parts of Europe, the Middle East and the western United States. However, these hydrological  
models often do not account for vegetation responses to rising atmospheric CO<sub>2</sub> and climate change.

55 Vegetation plays a crucial role within the global water cycle and thus impacts water availability for humans. Large-scale  
changes in vegetation type and coverage are already occurring due to climate change and human activities, such as  
deforestation. Vegetation plays a key role in precipitation generation, with approximately 60% of terrestrial precipitation  
originating from land via evapotranspiration – primarily through plant transpiration (Schneider et al., 2017; Wei et al., 2017).  
60 Vegetation also influences other hydrological processes, including infiltration, interception, and runoff (Caretta et al., 2022).  
Climate change continues to alter vegetation types and coverage globally, with increased vegetation growth in many regions  
(Xu et al., 2017; Yu et al., 2018; Zhu et al., 2016), but greater plant stress and mortality due to droughts and heatwaves in  
others (Parmesan et al. 2022).

65 Rising atmospheric CO<sub>2</sub> concentrations also impact the water cycle by altering plant physiology. Plants continuously adjust  
the widths of their stomatal openings to maximise photosynthesis while minimising water loss (Cowan, 1978). Under higher  
atmospheric CO<sub>2</sub>, plants typically reduce their stomatal openings, as they can maintain higher rates of photosynthesis at  
increased leaf-level water-use efficiency, thereby decreasing transpiration (Battipaglia et al., 2013; Field et al., 1995; Norby  
and Zak, 2011). As less water is lost through transpiration, more water remains in the soil and at the surface, contributing to  
70 increased runoff and soil moisture levels (Fowler et al., 2019; Gedney et al., 2006). However, higher CO<sub>2</sub> generally enhances  
photosynthesis, known as the CO<sub>2</sub> fertilisation effect, which promotes vegetation growth. This expansion in leaf area can  
increase canopy transpiration through a greater number of stomata, even though stomatal openings are individually reduced  
(Betts et al., 1997). At the canopy-scale, the resulting increase in vegetation water demand can offset, or even reverse, the  
runoff increases associated with reduced stomatal openings (Cowling and Field, 2003; Piao et al., 2007; Ukkola et al., 2016).  
75 The net effect on canopy transpiration thus depends on the balance between reduced stomatal openings and increased  
vegetation growth, which varies among plant species and climatic biomes (Norby and Zak 2011).

Better understanding of vegetation-water-atmosphere interactions, in both historical observations and under future climate  
change scenarios (e.g., Betts et al., 2007; Gedney et al., 2006) has been made possible with the introduction of Land Surface  
80 Models (LSMs). LSMs simulate complex interactions between the atmosphere, land surface, and sub-surface, including energy  
and water fluxes, carbon cycling, and soil processes. Dynamic vegetation schemes in LSMs have been made increasingly  
realistic over the past few decades (Fisher and Koven, 2020). They typically simulate vegetation coverage, canopy height and  
leaf area index for a limited number of generalised plant functional types, driven by carbon fluxes and vegetation competition.  
Including dynamic vegetation in climate models is essential for capturing critical changes in land surface and plant physiology  
85 that influence the climate system and hydrological cycle. Yet these schemes are still absent from many hydrological models.

Advances in LSMs have improved understanding of how plant stomatal and structural responses to rising CO<sub>2</sub> impact the  
water cycle. An early study by Wigley and Jones (1985) was one of the first to link CO<sub>2</sub>-driven changes in plant  
evapotranspiration (ET) to runoff. As land surface and climate models have advanced, effects of CO<sub>2</sub>-induced vegetation  
90 growth on the water cycle have also been analysed alongside stomatal closure. Betts et al. (1997) projected that increased  
vegetation cover could partially offset the projected reduction in ET due to increased stomatal closure. Gedney et al. (2006)  
attributed rising historical continental river runoff records to CO<sub>2</sub>-induced stomatal closure. However, Piao et al. (2007)  
suggested that when CO<sub>2</sub>-induced leaf area increases were also considered global runoff *reduced* from 1901 to 1999.  
Subsequent modelling studies have also concluded that CO<sub>2</sub>-induced stomatal closure and leaf area increases together generally  
95 *increase* projected global runoff in the current generation of models. For instance, doubling CO<sub>2</sub> in climate models led to  
global mean runoff increases of 6% (Betts et al., 2007) and 8-9% (Cao et al., 2010) relative to preindustrial; increases that are  
comparable to that simulated in response to radiatively forced climate change in both studies. Further studies have suggested  
that stomatal and structural responses to rising CO<sub>2</sub> affect the hydrological cycle differently around the globe. These studies

generally suggested increased runoff and streamflow, especially in the tropics (Davie et al., 2013; Fowler et al., 2019; Lemordant et al., 2018; Yang et al., 2019), reduced drought severity (Swann et al., 2016) and increased flood risk (Kooperman et al., 2018). Conversely, studies have suggested that CO<sub>2</sub>-induced vegetation structural responses exacerbate drying in more arid locations, including the mid-latitudes, in modelling projections (Fowler et al., 2019; Lemordant et al., 2018; Mankin et al., 2019) and observations (Ukkola et al., 2016). Moreover, observed streamflow shows limited sensitivity to the stomatal and structural responses to increased CO<sub>2</sub> (Wei et al., 2024). However, at the global scale, studies typically suggest that CO<sub>2</sub>-induced stomatal responses have a greater influence on runoff and streamflow than CO<sub>2</sub>-induced vegetation structural responses, particularly in future climate projections (e.g., Betts et al., 2007; Cao et al., 2010; Lemordant et al., 2018).

Only a few studies have examined how vegetation stomatal and structural responses to rising CO<sub>2</sub> influence human impacts of water scarcity. Wiltshire et al. (2013a,b) suggested that including this response could reduce the global population living under high water stress by approximately 200 million by 2100. Furthermore, a multi-model assessment by Wang and Sun found that vegetation–CO<sub>2</sub> feedbacks introduce systematic biases in projected extreme drought frequency, leading to underestimations of exposed population (5.25%) and GDP (6.07%) in the 2030s, but overestimations of ~3–9% for population and ~3–7% for GDP by the 2050s.

Together, these findings highlight the important influence of CO<sub>2</sub>-induced vegetation responses on the socioeconomic impacts of water scarcity. This study is the first to quantify these influences by replicating the design of typical hydrological impact studies - running a standalone impact model with fixed dynamic vegetation driven by climate model output - and adjusting the different vegetation responses to rising CO<sub>2</sub> and climate change. This approach allows us to estimate how incorporating these vegetation responses alters estimates of water scarcity in conventional impact studies.

## 120 **2 Methodology**

### **2.1 Experimental design**

The experimental setup is designed to replicate the framework commonly used in water-related impact studies, in which a hydrological model is run standalone and driven by climate model output. This framework is widely adopted because it is much more computationally efficient than running fully coupled ESMs, enabling higher resolution simulations and experiments in which specific processes can be systematically switched on and off. By applying this framework with a land surface model, we are able to directly assess how the inclusion of plant stomatal and structural responses to rising CO<sub>2</sub> and climate change alters conventional water scarcity projections. However, running models offline can introduce inconsistencies with the driving climate model, as discussed in Section 4.

130 Here we use the Joint UK Land Environment Simulator (JULES; Best et al., 2011; Clark et al., 2011) as the offline impact  
model, as it includes both a global hydrological cycle and dynamic vegetation scheme (Cox, 2001). JULES enables the  
isolation of vegetation stomatal and structural responses to rising CO<sub>2</sub> and climate change in order to investigate their  
influence on the hydrological cycle. JULES has been driven by the bias-adjusted (following Lange, 2019) Earth system  
climate model HadGEM2-ES (Hadley Centre Global Environment Model version 2; Jones et al., 2011) resampled to 0.5 x  
135 0.5 degrees horizontal resolution as part of the bias correction. We use the historic simulation from 1861 to 2005 and the  
“future” period 2006 to 2100 using Representative Concentration Pathway (RCP) 6.0. The earth system configuration  
JULES-ES is used following the setup for the Inter-Sectoral Impact Model Intercomparison Project (ISIMIP;  
<https://www.isimip.org/>) version 2b; details of the setup can be found in Mathison et al. (2023).

140 Four JULES simulations were performed by selectively fixing or allowing variation in the following two components:

- (1) **Atmospheric CO<sub>2</sub>:** Fixed (in JULES only) to 277ppm to represent preindustrial levels following protocol of the  
TRENDY project (Sitch et al., 2024).
- (2) **Vegetation structure:** The spatial and temporal vegetation distribution, including Leaf Area Index (LAI; the ratio of  
leaf to ground area), fixed in JULES to its initial state.

145

Simulations follow the naming convention <forcing>: <response>, where CLIM denotes climate changes, CO<sub>2</sub> atmospheric  
CO<sub>2</sub> changes, STOM stomatal responses, and VEG vegetation cover and leaf area responses (Table 1; see Table A1 for full  
details). S1 (CLIM: STOM) includes climate-driven stomatal responses only, with fixed vegetation, representing a typical  
offline hydrological model configuration. S2 (CLIM: STOM+VEG) additionally includes climate-driven vegetation changes.  
150 S3 (CLIM+CO<sub>2</sub>: STOM) includes both climate- and CO<sub>2</sub>-driven stomatal responses, while S4 (CLIM+CO<sub>2</sub>: STOM+VEG)  
includes all climate- and CO<sub>2</sub>-driven effects on stomata and vegetation, approximating a fully coupled Earth system model.

Process contributions or “isolated factors” are diagnosed from differences between simulations. CLIM: VEG (S2–S1)  
represents climate-induced structural vegetation response, CO<sub>2</sub>: STOM (S3–S1) represents CO<sub>2</sub>-induced stomatal response,  
155 CO<sub>2</sub>: STOM+VEG (S4–S2) represents CO<sub>2</sub>-induced stomatal and vegetation response, and CO<sub>2</sub>: STOM & CLIM+CO<sub>2</sub>: VEG  
(S4–S1) represents the total of CO<sub>2</sub>-induced stomatal response plus climate- and CO<sub>2</sub>-induced vegetation structural responses.  
The final factor (S4–S1) represents the difference between a typical hydrological impact study and fully coupled Earth system  
model. Relative differences (Figs. 2, 4, 8 and 9) are calculated as (b–a)/a. Note that we do not analyse the influence of climate  
change alone in this study.

160

**Table 1: Details of dynamic processes included in each of the simulations and isolated factors.**

Simulation	Name	Climate-induced stomatal changes	Climate-induced veg. changes	CO <sub>2</sub> -induced stomatal changes	CO <sub>2</sub> -induced veg. changes
S1	CLIM: STOM	✓			
S2	CLIM: STOM+VEG	✓	✓		
S3	CLIM+CO <sub>2</sub> : STOM	✓		✓	
S4	CLIM+CO <sub>2</sub> : STOM+VEG	✓	✓	✓	✓
S2 - S1	CLIM: VEG		✓		
S3 - S1	CO <sub>2</sub> : STOM			✓	
S4 - S2	CO <sub>2</sub> : STOM+VEG			✓	✓
S4 - S1	CO <sub>2</sub> : STOM & CLIM+CO <sub>2</sub> : VEG		✓	✓	✓

For all simulations, the atmospheric CO<sub>2</sub> and meteorological input variables such as radiation, temperature, precipitation and windspeed, are identical, since they come from the driving climate model HadGEM2-ES output, as would be the case for a typical hydrological study. Furthermore, all simulations use atmospheric CO<sub>2</sub> concentrations from the driving climate model (RCP 6.0), noting that, in the preindustrial CO<sub>2</sub> simulation, atmospheric CO<sub>2</sub> has been fixed in JULES only and not the driving climate input data. Note that anthropogenic disturbance of land is not included in any of the simulations, so vegetation can be affected by changes in climate and CO<sub>2</sub> only. Some of the meteorological inputs from HadGEM2-ES are shown in Fig. 1.

170

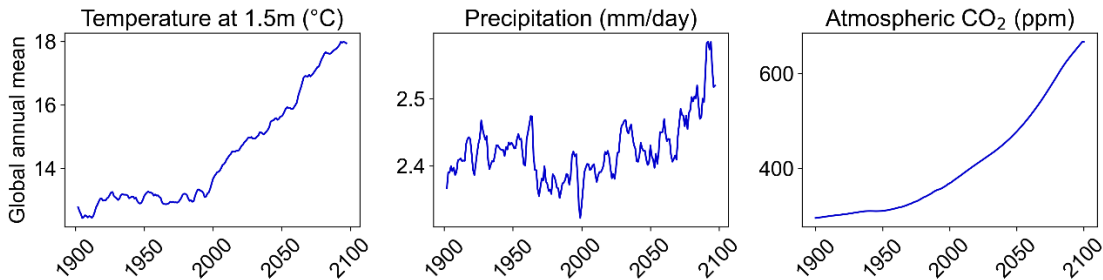
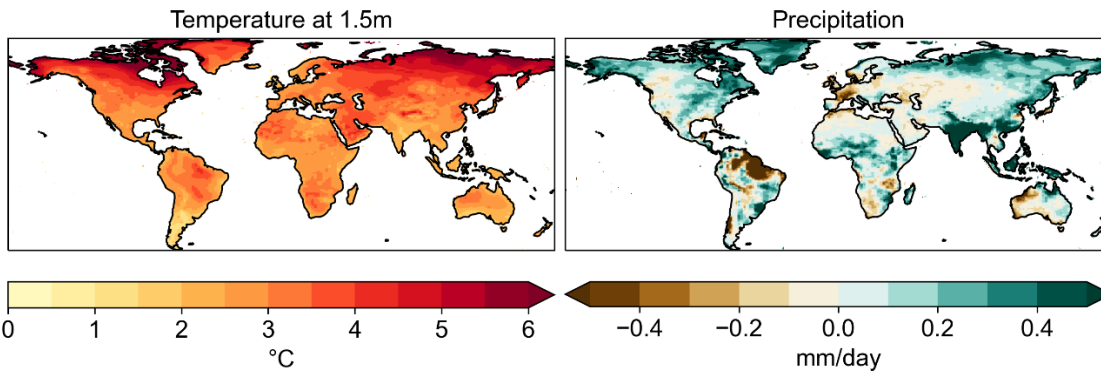


**Figure 1a: Global annual mean timeseries for climate variables from driving climate model HadGEM2-ES used as input to JULES simulations (rolling 5-year mean for precipitation and temperature).**



175

**Figure 1b: Mean changes from present (2006-2025) to future (2076-2095) for 1.5m temperature (left) and precipitation (right) from driving climate model HadGEM2-ES used as input to JULES simulations.**

Using the output from the four simulations in Table 1, we investigate the influence of the different vegetation responses on  
 180 global water scarcity. We calculate the Water Scarcity Index (WSI) as the ratio of water demand to water supply  
 (Falkenmark et al., 1989). The WSI has been chosen as it is a simple and widely used indicator of water scarcity. We use a  
 WSI of 0.2-0.4 to indicate mild or emerging water scarcity, and  $WSI \geq 0.4$  for severe water scarcity, in line with Raskin and  
 Gleick (1997) and Greve et al. (2018). Runoff is used as a proxy for water supply because it represents the fraction of  
 185 precipitation that is not lost to evapotranspiration and is therefore available for water resources. Total runoff is taken from  
 the output of the simulations and includes both surface (overland flow generated when precipitation exceeds infiltration  
 capacity or soil saturation) and sub-surface runoff (lateral drainage through the soil column) at the grid box scale. Water  
 demand has been downloaded from the ISIMIP database (<https://data.isimip.org/>), specifically ISIMIP2b from the global  
 water sector (Gosling et al., 2023). The hydrological model used is H08 (Hanasaki et al., 2008a, b, 2018) driven by  
 HadGEM2-ES, RCP 6.0 and shared socioeconomic pathway SSP2, which represents population and gross domestic product  
 190 for the ‘middle of the road’ scenario (Riahi et al., 2017). Total water demand is represented by summing water withdrawal  
 for irrigation (assuming unlimited water supply), domestic use and manufacturing.

Different approaches can be used to calculate the average WSI over space and time, which can considerably influence the  
 results. Mostly, we have chosen to calculate WSI at the most granular spatial and temporal scale, which is monthly and by  
 195 grid-box. The exception is when analysing by river basins in Figs. 8 and 9, where the sum of total supply and demand is  
 computed for each basin before calculating WSI. The rationale is that, generally, all water within a river basin could ideally  
 be used for all the population within that basin, noting in real life this is not always the case.

Since WSI is calculated as water demand divided by water supply, it can yield extremely high values where supply values are  
 200 very low relative to demand. To moderate the impact of these extreme values, the *median* WSI is used for spatial and temporal

averaging in this study, as it provides a more robust measure less influenced by outliers. Additionally, median WSI is calculated over larger spatial areas. Firstly, by the climate regions outlined in the Intergovernmental Panel on Climate Change (IPCC) Sixth Assessment Report (AR6), consisting of 46 land regions based on a combination of geographic, climatic, and socio-economic criteria (Fig. S2; Iturbide et al., 2020). Secondly, by Hydrosheds river basins (https://www.hydrosheds.org/products/hydrobasins; Lehner and Grill, 2013).

Finally, population projections are for SSP2 from the ISIMIP2b data library (Piontek and Geiger, 2017), plotted in Fig. S1, which are gridded at 0.5 x 0.5-degree resolution. These have been used to calculate projected population numbers by river basin in Table 2 and Fig. 8.

## 2.2 The Joint UK Land Environment Simulator (JULES)

JULES is a process-based model simulating fluxes of carbon, water, energy and momentum between the land surface and atmosphere. JULES is used as either an integral part of an Earth System Model such as UKESM1 (Sellar et al., 2019) or as an independent land surface model driven by input data from observations or atmospheric models; in this study it is used in the latter manner. JULES does not represent the same level of hydrological and water management detail as typically included in hydrological models; however, it does use a river routing scheme (Falloon et al., 2007), and, importantly for this study, has a dynamic vegetation model. The dynamic vegetation model predicts changes in leaf area and the fractional coverage of 13 different Plant Functional Types (PFTs; Harper et al., 2016) where each PFT is categorised by specific physiological traits, and surface fluxes are calculated separately for each PFT. JULES uses a coupled canopy conductance and photosynthesis model (Cox et al., 1998), based on Luening (1995), and TOPMODEL-type scheme to calculate soil moisture and runoff; more details on both are in Appendix B.

## 3. Results

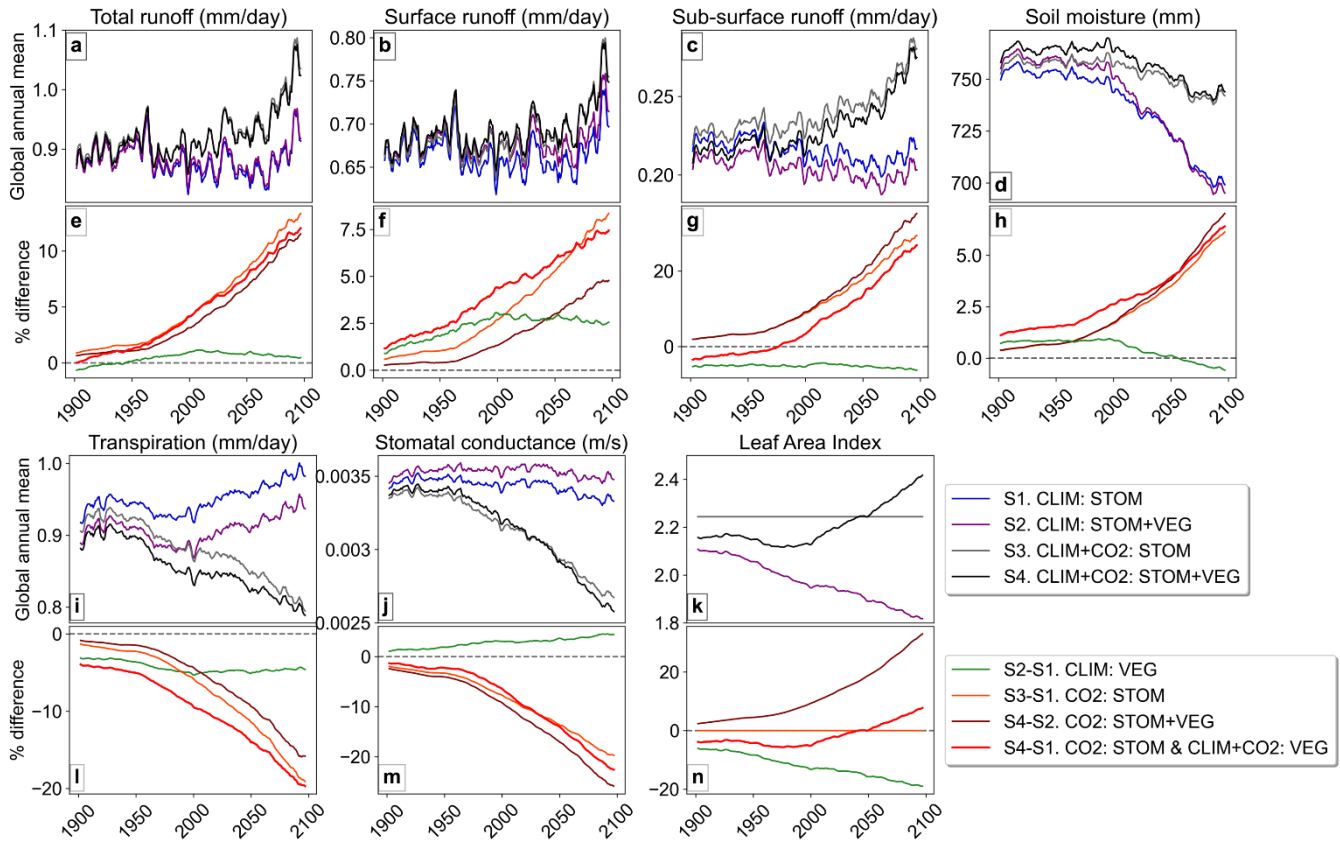
### 3.1 Vegetation and water cycle variables

The global-mean time series for water-cycle and vegetation variables (Fig. 2) reveal substantial divergence among simulations. The largest relative differences are associated with the CO<sub>2</sub>-induced stomatal response, as indicated by simulations including CO<sub>2</sub>: STOM, whose influence strengthens throughout the 21st century. In the climate-only simulation (S1), which reflects typical hydrological modelling approaches, soil moisture declines over the century while transpiration increases slightly (Fig. 2d,i), likely driven by rising temperatures (Fig. 1a).

In contrast, when the CO<sub>2</sub>-induced stomatal response is represented (S3 and S4), the projected soil-moisture decline is substantially muted, coincident with ~20% reductions in both transpiration and stomatal conductance by 2100 (Fig. 2l,m).

Despite decreasing soil moisture, total runoff in S1 shows a modest increase in the latter half of the century (Fig. 2a). This increase becomes ~10–12% larger when CO<sub>2</sub>-induced stomatal closure is included (Fig. 2e).

CO<sub>2</sub>-driven stomatal closure also dominates over the drying effect of CO<sub>2</sub>-driven increases in leaf area. In CO<sub>2</sub>: STOM+VEG, runoff continues to rise even with a ~30% increase in LAI (Fig. 2e,n). In contrast, climate-driven vegetation structural changes alone (CLIM: VEG) reduce LAI by ~20% (Fig. 2n), leading to a modest 3–5% reduction in transpiration (Fig. 2i) and only a slight enhancement in runoff (Fig. 2e).



240 **Figure 2: Global annual mean timeseries (rolling 5-year mean) in water cycle and vegetation variables in each simulation and the relative (%) difference between simulations.**

While the CO<sub>2</sub>-induced stomatal response contributes to overall surface wetting at the global scale (Fig. 2), its influence exhibits considerable spatial heterogeneity. Climate-driven runoff changes from the present (2006–2025) to the future (2076–2095) period are highly variable in both magnitude and direction (Fig. 3a) generally aligning with precipitation changes (Fig. 1b; right). When all vegetation responses are included in S4, the overall runoff and soil moisture pattern remain broadly similar

to the climate-only simulation S1 (Fig. 3a,b,e,f) though increases are more evident in some regions, particularly the tropics, largely due to CO<sub>2</sub>-induced stomatal closure. For instance, in CO<sub>2</sub>: STOM+VEG, runoff increases are projected in many regions (Fig. 3i), especially the tropics and high northern latitudes, corresponding with transpiration decreases (Fig. 3k). In areas with projected runoff decreases under climate forcing alone (Fig. 3a), such as in the Amazon, parts of the USA, northern and eastern Europe, the stomatal response mitigates drying and, in places such as central Africa, even *reverses* runoff decreases to increases (Fig. 3e).

In many regions, the CO<sub>2</sub>-induced combined vegetation response is driving runoff increases (Fig. 3i) despite CO<sub>2</sub>-induced LAI increases (Fig. 3l), suggesting that stomatal closure outweighs the drying effect of enhanced leaf area. However, the LAI increases appear to drive slight runoff reductions across some areas, particularly in semi-arid and arid climates such as the Middle East and western USA (Fig. 3i,l). Although considerably smaller than the increases, these small runoff reductions could cause significant impacts in already water-stressed areas. In contrast, climate-driven vegetation structural changes (CLIM: VEG) have relatively limited impact on runoff, soil moisture and transpiration, despite notable LAI changes in parts of the tropics and high latitudes (Fig. 3m-p).

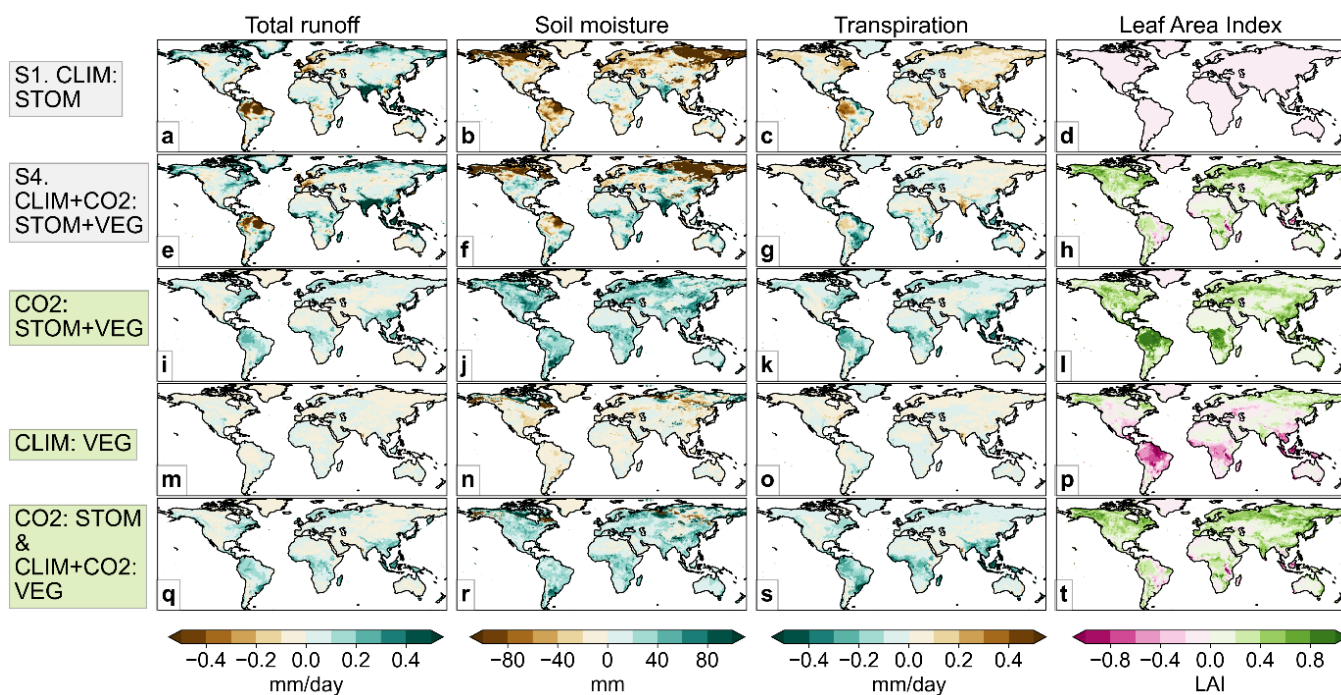


**Figure 3: Global mean changes from present (2006-2025) to future (2076-2095) period in the climate-only simulation (top row), and the absolute difference when the various isolated factors are included.**

265 **3.2 Water demand, supply and the Water Scarcity Index**

Global median water demand, supply, and WSI are projected to increase over the coming decades under SSP2 and RCP 6.0 (Fig. 4a-c). However, while water demand and WSI peak and subsequently decline later in the century, JULES projects a continued rise in global water supply, particularly in simulations S3 and S4 that include CO<sub>2</sub> effects on stomata (Fig. 4b). When the isolated effect of increased CO<sub>2</sub> on plant stomata is included (CO<sub>2</sub>: STOM), global median water supply is approximately 30% higher by 2100; even when CO<sub>2</sub>-induced structural changes are also included (CO<sub>2</sub>: VEG+STOM), supply is around 20% higher by 2100. In contrast, the climate effects on vegetation have a comparatively small influence on global median water supply, and this influence diminishes further in the coming decades (Fig. 4d; CLIM: VEG).

These water supply increases correspond with consistent projected reductions in global median WSI throughout the century (Fig. 4c,e). The CO<sub>2</sub>-induced stomatal response appears to ameliorate WSI by 15-20% toward the century-end shown by CO<sub>2</sub>: STOM (Fig. 4e). However, when CO<sub>2</sub>-induced LAI increases are also allowed in CO<sub>2</sub>: STOM+VEG, the reduction in WSI is notably less at 8-10% in the second half of the century. Climate-induced vegetation changes also reduce global median WSI by around 5%, remaining consistent throughout the period. When all processes are included, the combined influence shown by S4 – S1 (Fig. 4e) results in a 10-15% reduction in WSI throughout the century.

280

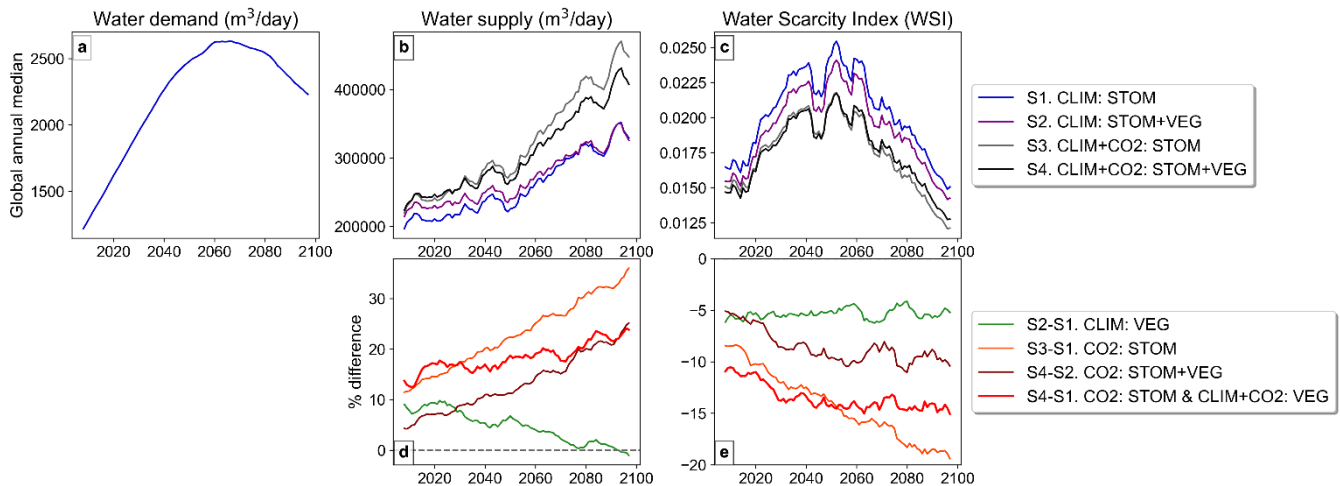


**Figure 4: Annual global-median timeseries (rolling 5-year mean) of a) water demand, b) water supply, c) WSI in the four simulations and the % difference in d) supply and e) WSI due to the various isolated factors. Note, water demand is the same across all simulations.**

285

Under RCP 6.0 and SSP2, water demand for the present period is high in much of Europe, South and Southeast Asia and the USA (Fig. 5a). Water demand increases for most places, especially in the highly populated and developing regions of South Asia, as well as parts of Africa, but decreases are also seen for parts of Europe and China (Fig. 6a). Regions experiencing

severe water scarcity ( $WSI \geq 0.4$ ; Raskin, et al., 1997) in the present period (2006 - 2025), include most of India, the Middle East, eastern China and parts of South Africa, USA, and Europe (Fig. 5c). Large swathes of northern Africa are also experiencing severe water scarcity despite low demand (Fig. 5a). Even though global median WSI reduces later this century in Fig. 4c, many of the already water scarce regions are projected to become even more water scarce by the future period (2076-2095; Fig. 6c), as the demand grows, including in highly populated regions such as India.

The plots comparing the change in median WSI from the present (2006-2025) to the future (2076-2095) under scenarios with and without plant processes (Fig. 6c,e) appear quite similar, suggesting that water demand and meteorological factors driving water supply are the primary influences on WSI. Interestingly, the changes in supply between the S1 and S4 simulations (Fig. 6b,d) show greater difference than those for WSI, since the supply differences mainly occur in areas with low levels of water scarcity, and therefore have less impact on WSI.

Despite the visual similarities between simulations with (Fig. 6e) and without (Fig. 6c) the combined vegetation responses to  $CO_2$  and climate change, the effect of plant responses on WSI is not negligible. The  $CO_2$ -induced stomatal response increases water supply in most regions, especially in the tropics (Fig. 6f), resulting in corresponding reductions in WSI (Fig. 6g). When  $CO_2$ -induced vegetation structural changes are also included in the  $CO_2$ : STOM+VEG simulations (Fig. 6h,i), overall supply still increases, as the supply reductions associated with  $CO_2$ -driven structural vegetation expansion are relatively small and less apparent in the plots. However, these modest reductions translate into substantial increases in WSI in arid regions such as the Middle East and northern and southern Africa (Fig. 6i), where baseline water supply is already low. Climate-induced vegetation changes shown in CLIM: VEG appear to have minimal impact on supply (Fig. 6j), yet there are substantial changes in WSI in some areas, with increases in some places, including western India, although parts of southern and northern Africa show some reductions (Fig. 6k). Finally, when all processes are combined in  $CO_2$ : STOM & CLIM+ $CO_2$ : VEG, supply predominantly increases (Fig. 6l), even though WSI increases in many arid and semi-arid regions.

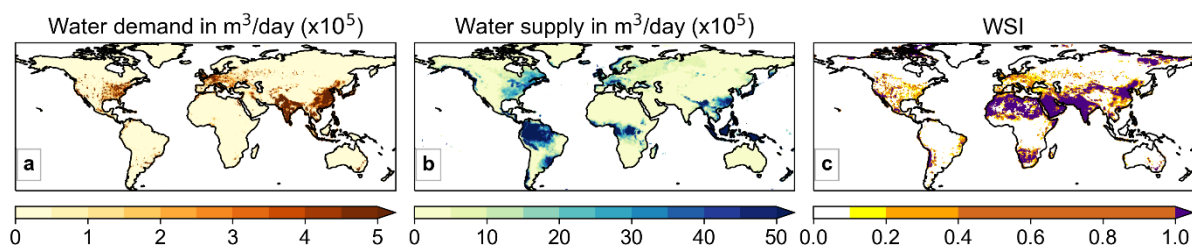
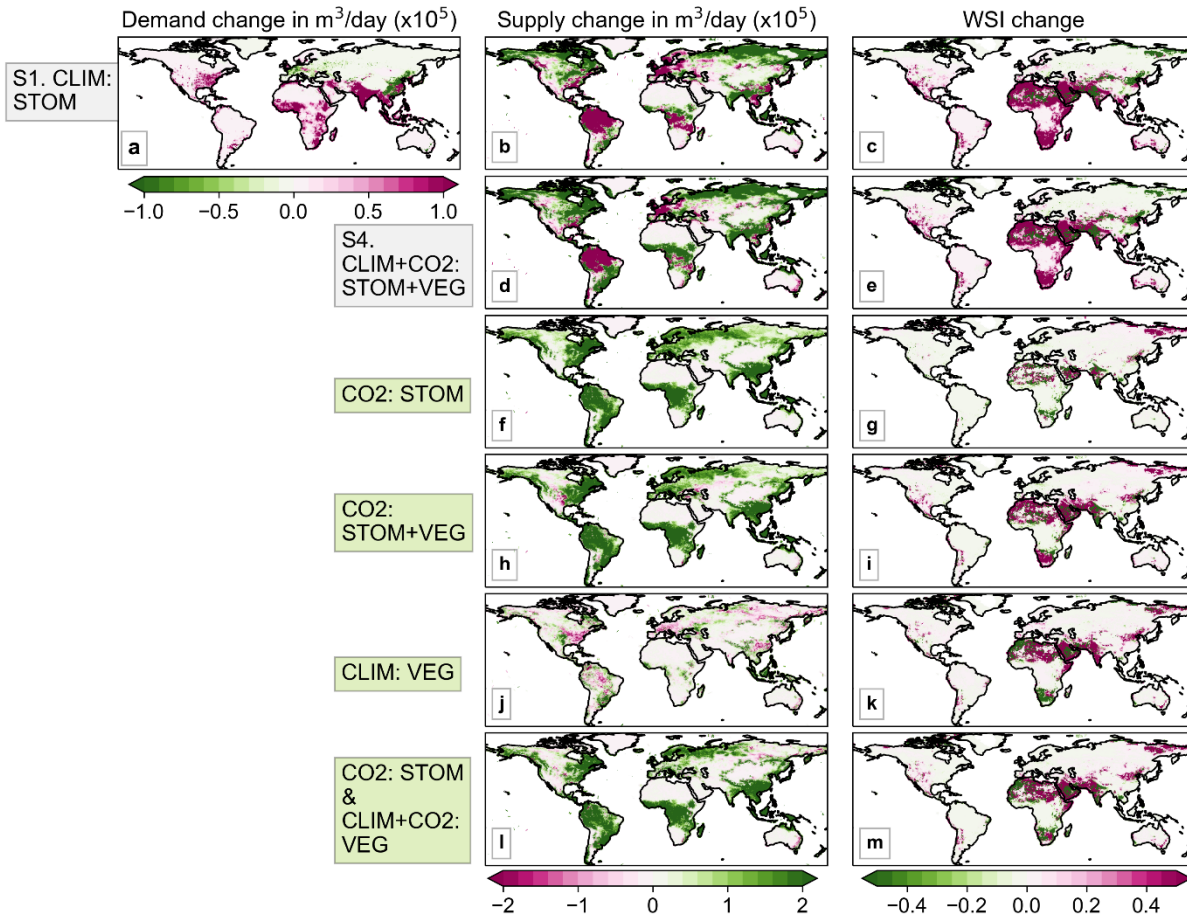


Figure 5: Median a) water demand, b) supply and c) Water Scarcity Index (WSI) for the period 2006-2025 in S1. CLIM: STOM.

315



**Figure 6: Median water demand, supply and Water Scarcity Index (WSI) change from the present (2006-2025) to future (2076-2095) period in simulations S1 and S4 (a-e), and the difference in supply and WSI when including the various isolated factors (f-m).**

320 The 25 IPCC AR6 climate regions with the highest monthly median WSI between 2076-2095 are shown in Fig. 7. The Arabian Peninsula region is projected to experience the highest median WSI, and South Asia is predicted to have the second highest (Fig. 7; left panel). Comparing with the 2006-2025 present period (Fig. S3), nearly all these regions are projected to increase in median WSI by the end of the century, with the largest increases in the East and West Southern Africa and Western Africa regions.

325

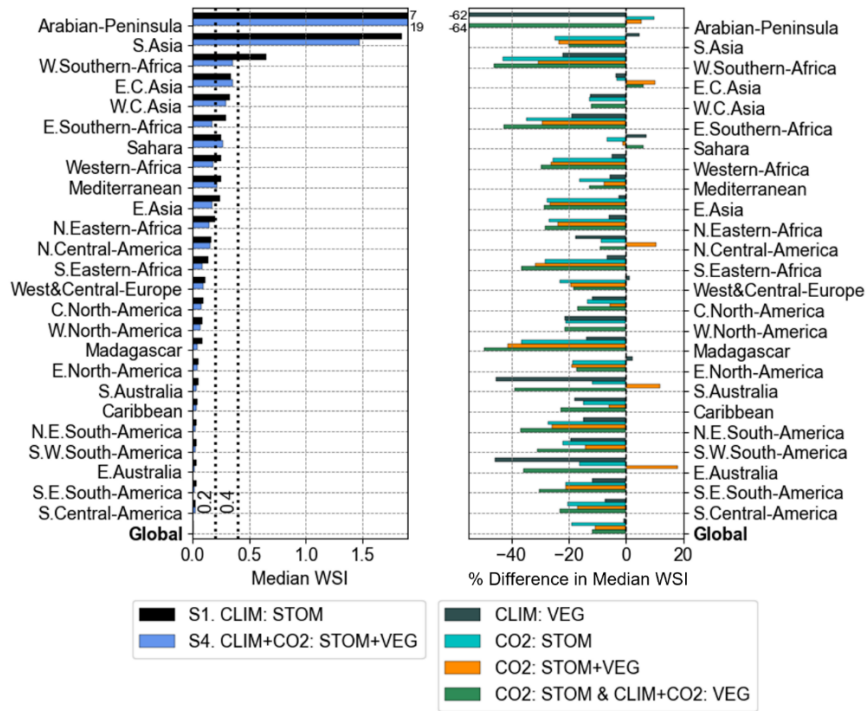
When all vegetation responses are included in S4, there is a reduction in median WSI for all regions, except for East Central Asia and the Sahara, when compared with S1 (Fig 8; left panel). The CO<sub>2</sub>-induced stomatal response appears to be driving the largest reductions in WSI, indicated by CO<sub>2</sub>: STOM and CO<sub>2</sub>: STOM+VEG (Fig. 7; right panel). Reductions of 30-40% are projected for Madagascar, East Southern Africa and South-Eastern Africa regions, and 20-30% reductions in Western Africa,

330 Northeast South America, and South and East Asia. These regions are predominantly in tropical climates, aligning with the areas of increased water supply shown in Fig. 6b. However, CO<sub>2</sub>: STOM+VEG also indicates increases in median WSI, potentially due to CO<sub>2</sub>-induced vegetation growth in regions like North Central America, East Central Asia, and South and East Australia. Climate-induced vegetation changes (CLIM: VEG) appear to drive WSI reductions in almost all regions, perhaps due to decreased leaf area and vegetation coverage requiring less water in these regions. These reductions are considerable in some areas, with ~45% decreases in East and South Australia. When all dynamic vegetation responses are considered in CO<sub>2</sub>: STOM & CLIM+CO<sub>2</sub>: VEG, the majority of these most water scarce regions see a 20-40% reduction.

335

These results are reinforced by alternative WSI measures; both the number of severely water scarce months (Fig. S4a) and % area in severe water scarcity (Fig. S4b), indicate that incorporating dynamic plant processes leads to a reduction in both the temporal and spatial extent of water scarcity for most regions. These reductions are also primarily driven by the CO<sub>2</sub>-induced reduction in stomatal aperture, particularly in the tropical regions such as East Asia and South-Eastern Africa.

340



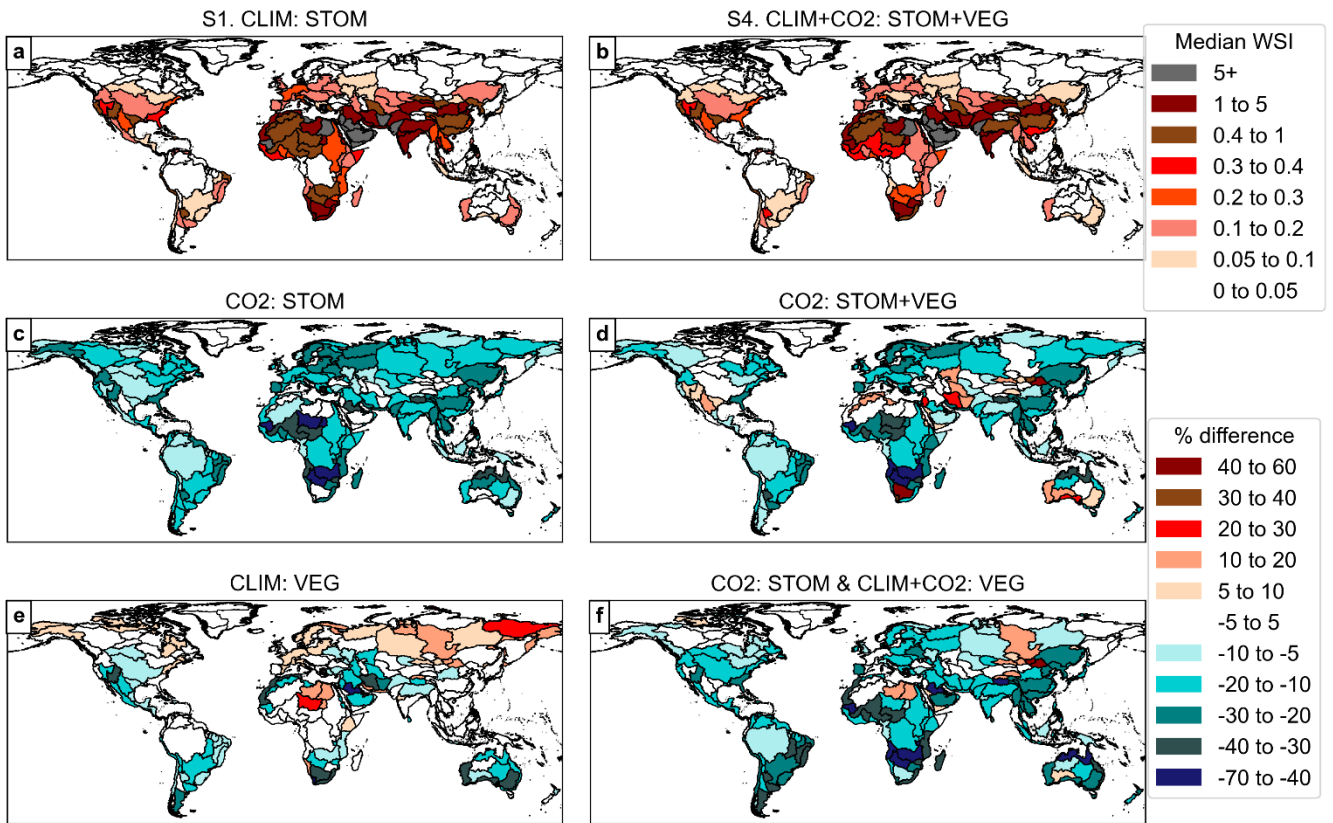
345 **Figure 7: Median monthly WSI in simulations S1 and S4 (left) and % difference of median WSI when including the various isolated factors (right) by IPCC AR6 regions for the future period 2076-2095. The grey dashed lines (left) indicate the thresholds for mild water scarcity (WSI  $\geq$  0.2) and severe water scarcity (WSI  $\geq$  0.4). Only the 25 regions with the highest median WSI, according to the S1. CLIM: STOM simulation, are shown, sorted from the most water scarce region (top) to the least (bottom). The global median is also presented at the bottom. Out-of-range values for the Arabian-Peninsula are printed at the top.**

350 When analysing median WSI by river basins for the future period (2076 – 2095; Fig. 8), the findings become clearer compared to the grid-cell analysis in Fig. 6. Similar to the bar plots in Fig. 7, the comparison of median WSI between scenarios S1 and S4 (Fig. 8a, b) suggests that dynamic plant processes results in limited overall changes. However, WSI category shifts are suggested for several basins, including in central, southern, and northern Africa, Southeast Asia, and eastern Australia. Supporting our existing findings, the CO<sub>2</sub>-induced stomatal response reduces WSI in many basins (Fig. 8c,d,f); median WSI  
355 at least 20% lower in numerous basins, including in Europe, central and southern Africa, and South and East Asia, and at least 40% lower in basins in part of Africa. When CO<sub>2</sub> effects on vegetation structure are also included in CO<sub>2</sub>: STOM+VEG, median WSI increases by more than 10% in 18 basins (Table 2) including in the Middle East, Australia, Southern and Northwestern Africa, and the western USA (Fig. 8d), potentially due to CO<sub>2</sub>-induced vegetation structural increases enhancing drying. However, the supply increases from stomatal responses due to enhanced CO<sub>2</sub> appear to dominate, resulting in WSI  
360 reductions by at least 10% in 122 basins (Table 2).

The effects of climate-induced vegetation structural changes are more varied with modest increases in WSI (<10%) in much of Europe and larger increases (10-30%) in central-northern Africa. However, reductions are more common, particularly around arid and semi-arid regions (Fig. 8e), also supported by Table 2, which suggests more increases than decreases in median  
365 WSI across all the thresholds.

Considering all factors combined (CO<sub>2</sub>: STOM & CLIM+CO<sub>2</sub>: VEG), decreases in WSI outweigh increases (Fig. 8f). Out of 291 basins, 139 show reductions of at least 10% (maximum 67%), affecting 80% of the global population, while only 11 basins see increases over 10% (maximum 59%), affecting just 0.2% of the population (Table 2). Most of the population are seeing  
370 small percentage changes compared with large ones, shown by the higher numbers in the lower thresholds (e.g., 5% and 10%) in Table 2. For example, when all processes are included in CO<sub>2</sub>: STOM & CLIM+CO<sub>2</sub>: VEG, median WSI will reduce by at least 5% for 88% of the population compared with reductions of at least 40% for only 2% of the population.

Figure S5 shows the number of months in severe water scarcity (WSI  $\geq$  0.4), with the CO<sub>2</sub>-induced stomatal response again driving small reductions of mainly 1 to 2 months in many basins, in similar regions to those seen in Fig. 8f, including southern South America, central and southern Africa southeast Asia and coastal Australia. The results are also consistent when dividing into seasons, which show overwhelming reductions in median WSI across all seasons in the future period (Fig. S6).  
375



380 **Figure 8: Median WSI in simulations S1 and S4 (top row) and the relative (%) difference in median WSI when including the various isolated factors by river basin for the future period 2076-2095.**

	<b>Threshold (%)</b>	<b>Factor</b>	<b>Basin count above Threshold</b>	<b>Basin count below -Threshold</b>	<b>Percentage of population above Threshold</b>	<b>Percentage of population below -Threshold</b>
385	<b>5</b>	CO2: STOM	0	198	0.0	90.1
		CO2: STOM+VEG	26	169	4.4	83.5
		CLIM: VEG	51	76	7.3	33.4
		<b>CO2: STOM &amp; CLIM+CO2: VEG</b>	<b>17</b>	<b>176</b>	<b>1.1</b>	<b>87.8</b>
390	<b>10</b>	CO2: STOM	0	156	0.0	81.4
		CO2: STOM+VEG	18	122	2.7	62.0
		CLIM: VEG	21	43	0.4	9.3
		<b>CO2: STOM &amp; CLIM+CO2: VEG</b>	<b>11</b>	<b>139</b>	<b>0.2</b>	<b>80.2</b>
395	<b>20</b>	CO2: STOM	0	67	0.0	24.7
		CO2: STOM+VEG	7	56	1.0	21.4
		CLIM: VEG	5	15	0.1	2.6
		<b>CO2: STOM &amp; CLIM+CO2: VEG</b>	<b>4</b>	<b>68</b>	<b>0.0</b>	<b>26.4</b>
400	<b>40</b>	CO2: STOM	0	9	0.0	1.6
		CO2: STOM+VEG	2	6	0.3	1.9
		CLIM: VEG	1	2	0.0	0.2
		<b>CO2: STOM &amp; CLIM+CO2: VEG</b>	<b>3</b>	<b>11</b>	<b>0.0</b>	<b>2.1</b>

**Table 2. Total number of river basins and the percentage of the total projected global population affected by changes in median WSI relative to specific percentage thresholds, driven by various isolated factors for the period 2076–2095.**

The annual cycles of median WSI for the period 2076 to 2095 across several major river basins are illustrated in Fig. 9, along with the relative differences when the isolated factors are included. These basins were selected based on their population and water scarcity levels, ensuring a fair geographic distribution across all continents (excluding the poles).

All basins experience periods of water scarcity during parts of the year. Consistent with previous findings, the inclusion of the CO<sub>2</sub>-induced stomatal response mitigates WSI in all basins throughout the year, and especially during water-scarce periods. In some basins, this effect reduces WSI by over 40% during certain times of the year. For instance, in the northwest Africa and Tigris-Euphrates basins (Fig. 9a,c), the WSI is projected to be at least 50% lower during the most water-scarce periods. The basin in southern Africa presents contrasting results to the other basins and to our existing results; when including the CO<sub>2</sub>-induced vegetation structural increases in CO2: STOM+VEG, median WSI is 50% higher, which is the case for much of the year. Interestingly, climate-induced vegetation structural changes drive 40-50% reduction in WSI over the year. These two processes appear to be balancing one another out, as the combined effect of all processes results in minimal net change in WSI.

Overall, including all vegetation responses to CO<sub>2</sub> and climate change in S4, consistently mitigates WSI across the year in most basins, with the magnitude of these effects varying across the year. These findings suggest that the combined vegetation responses have the most substantial impact during periods of water scarcity, highlighting their importance in future water scarcity projections.

420

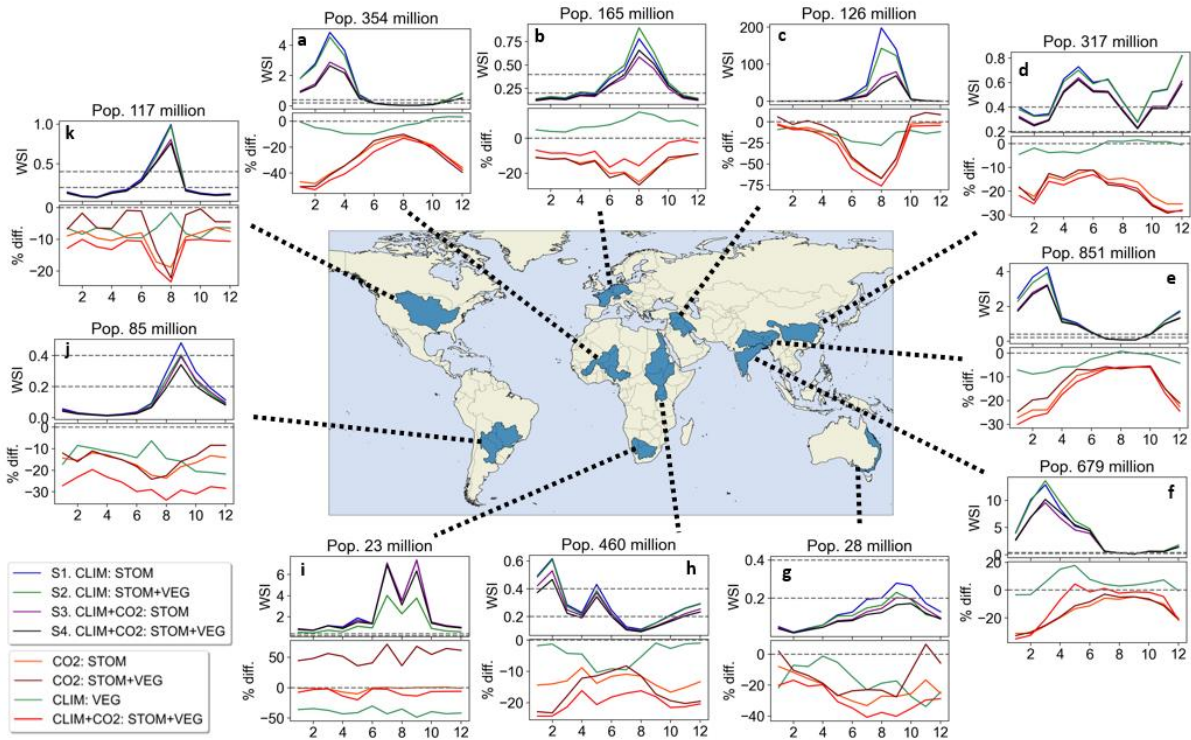


**Figure 9: Annual cycles of median WSI, and the relative (%) difference in median WSI when including the various isolated factors for various river basins around the world for the future period 2076-2095. Total population of the basin is noted above each plot.**

#### 425 4 Discussion

Existing studies on the socioeconomic impacts of water scarcity are typically based on hydrological models that do not include vegetation stomatal or structural responses to rising CO<sub>2</sub> and climate change (e.g., Dolan et al., 2021; Gosling and Arnell, 2016; Greve et al., 2018; Haddeland et al., 2014; Schewe et al., 2013). By replicating the common approach, i.e., driving a standalone impacts model with climate model output, this study investigates the influence of incorporating these plant responses in such analyses.

430

Numerous observational and modelling studies have demonstrated the impact of the CO<sub>2</sub>-induced stomatal and structural responses on the water cycle. In line with many of these studies (e.g., Betts et al., 2007; Cao et al., 2010; Gedney et al., 2006),

our results suggest that, for the overall global mean, rising CO<sub>2</sub> decreases stomatal conductance and transpiration, leading to  
435 higher soil moisture and increased runoff (Figs. 2 and 3). Projected total runoff increases of 10-12% by the end of the century  
(Fig. 2e) are analogous with the global mean values suggested in Betts et al. (2007) and Cao et al. (2010). The runoff increases  
from the stomatal response are most pronounced in the tropics (Fig. 3i), corroborating the findings of several studies (e.g.,  
Davie et al., 2013; Fowler et al., 2019; Lemordant et al., 2018; Yang et al., 2019). Furthermore, also supported by these studies,  
our results suggest that global mean LAI increases with rising CO<sub>2</sub> (Fig. 2k,n), but, at the global scale, any reductions in runoff  
440 due to increased vegetation cover and LAI is outweighed by the increases in runoff due to the CO<sub>2</sub>-induced stomatal response,  
since CO<sub>2</sub>: STOM+VEG shows relative *increases* for global mean runoff and soil moisture (Fig. 2e-h). However, CO<sub>2</sub>- and  
climate-induced vegetation increases are still projected to drive small decreases in runoff across large areas of the globe,  
especially semi-arid and arid regions, west USA, parts of mid-latitudes and Australia, supported by several studies (e.g., Piao  
et al., 2007; Ukkola et al., 2016). Even though these decreases appear negligible in number, water supply is already low in  
445 many of these regions and therefore a small decrease can greatly exacerbate water scarcity in these areas.

The increase in global runoff and thus water supply when all the plant responses are included in our simulations translates to  
reductions in global median WSI. Our results suggest that the wetting effect of the stomatal response to rising CO<sub>2</sub> has the  
dominating influence over the drying effect of increased vegetation structural response in most places, especially when  
450 aggregated by IPCC climate regions and river basins. Under RCP 6.0 and SSP2 “middle-of-the-road” scenarios, global median  
WSI increases until mid-century and then declines (Fig. 4c), although many places will still experience worsening water  
scarcity throughout the century (Fig. 6c). Water scarcity projections with and without dynamic plant processes (Figs. 6-8) do  
not present drastic differences, but the influence of plant responses, particularly the stomatal response to rising CO<sub>2</sub>, still have  
a noticeable effect when the results are collated over larger areas. In most IPCC AR6 regions and river basins, median WSI is  
455 *lower* when all plant responses are included in CO<sub>2</sub>: STOM & CLIM+CO<sub>2</sub>: VEG (Figs. 7-8; Table 2). Although CO<sub>2</sub>-induced  
stomatal closure substantially increases water supply by ~35% (Fig. 4d), it reduces WSI by only ~20% (Fig. 4e) by 2100. The  
smaller influence on WSI arises because the largest supply increases are due to the CO<sub>2</sub>-induced stomatal response, which has  
most influence in non-water scarce regions with abundant water supply, such as tropical regions like the Amazon and Southeast  
Asia (Fig. 6f,g), which contribute less to WSI values.

460 Notable differences emerge when computing WSI at different spatial scales. At the grid-box level, plant responses often lead  
to increases in median WSI across many areas (Fig. 6), because local demand, particularly in urban areas, can often  
substantially exceed local supply, as runoff from surrounding grid-boxes is not accounted for. In contrast, at larger spatial  
scales, decreases in WSI are more common (Figs. 7 to 9), as aggregating supply and demand across broader areas generally  
465 lowers WSI. For river basins, total runoff is assumed to be accessible to all inhabitants within the basin, which smooths out  
local imbalances. While neither approach fully captures the complexity of water distribution and accessibility, this is not a

critical limitation for this study, which is to assess the *relative* influence of vegetation responses on WSI rather than produce precise estimates.

470 Furthermore, our findings may overestimate WSI in places, as our proxy for water supply is total runoff estimated using  
JULES, which does not include some sources which can supplement water supply, such as groundwater extraction. Another  
consideration which could mean our WSI estimates are too high, is because water demand for irrigation is estimated by  
hydrological model ‘H08’, which, like many other hydrological models, does not account for vegetation structural or stomatal  
responses to rising CO<sub>2</sub> and climate change. Additional atmospheric CO<sub>2</sub> generally makes crops more water-efficient, lowering  
475 water required for irrigation, and thus potentially alleviating water scarcity.

The HadGEM2-ES climate data driving JULES in this study has been bias-corrected following the ISIMIP2b protocol,  
although some residual biases remain in the JULES version used (Mathison et al., 2023). For 1980–2006, their evaluation  
indicates negligible runoff biases for most river basins. However, slight runoff underestimations in China and the northern  
480 high latitudes translate to overestimations in WSI in our study. Conversely, slight runoff overestimations in eastern USA  
translate to underestimations in WSI in our study. To assess the influence of plant responses, we take the difference between  
two simulations that share similar biases, and thus this minimises overall biases. Non-linear biases may persist when comparing  
simulations with differing plant responses, but these are expected to be relatively small compared with other uncertainties  
inherent in such modelling studies.

485 JULES uses parameterisation schemes to represent hydrological and biophysical processes. For example, the stomatal  
conductance scheme (see Appendix B) simplifies a complex process which varies across species, ecosystems, and climates  
(Norby and Zak, 2011). Evaluating the accuracy of such parameterisation schemes on a global scale is a major challenge,  
primarily due to limited observational data. Experiments such as Free Air CO<sub>2</sub> Enrichment (FACE) have provided valuable  
490 insights into plant physiological responses to elevated CO<sub>2</sub>, which are crucial for land surface model developments, but are  
currently at a small number of point locations. Model-data comparison studies suggest mixed performance at simulating CO<sub>2</sub>  
effects on water-use efficiency, with models performing well for some sites and species but poorly for others (De Kauwe et  
al., 2013; Walker et al., 2014). Although JULES has not yet been comprehensively assessed in these studies, its behaviour is  
expected to be broadly comparable to the models evaluated. Furthermore, some studies suggest that the magnitude of the CO<sub>2</sub>-  
495 effect on river runoff records in JULES is reasonable within uncertainty bounds (Gedney et al., 2006, 2014).

Since only one land surface model was assessed in this study, further work could test additional models to examine the  
sensitivity of the results. We would anticipate broadly consistent outcomes across LSMs when testing the stomatal response,  
as many LSMs employ stomatal conductance parameterisation schemes derived from similar formulations. However, we  
500 would expect a wider spread of responses in LSMs when testing vegetation structural responses, given that different Dynamic

Global Vegetation Models apply alternative approaches to dynamic vegetation compared with the TRIFFID scheme used in JULES (Sitch et al., 2008).

505 Finally, we recognise that, to mimic typical hydrological impact studies, JULES was run standalone driven by climate model output, without feedbacks to the driving climate model. For example, disabling the stomatal response to rising CO<sub>2</sub> in JULES typically increases transpiration (Fig. 2), which typically enhances atmospheric moisture affecting humidity, temperature, and precipitation. Such feedbacks could amplify differences in water scarcity projections between simulations with and without vegetation responses. Assessing the importance of these missing interactions could highlight the value of using hydrological models coupled to the atmosphere for water scarcity assessments.

## 510 **5 Conclusions**

Our results suggest that including plant stomatal and structural responses to rising CO<sub>2</sub> and climate change in JULES partially moderates water scarcity in many regions throughout this century. CO<sub>2</sub>-induced stomatal closure enhances water-use efficiency, increasing water availability, particularly in the tropics. The supply increase translates to decreases in WSI in many regions, although the largest increases in water supply occur in regions that already experience abundant rainfall, such as the 515 tropics, which typically do not experience water scarcity. As a result, globally averaged reductions in WSI due to stomatal responses are smaller than the corresponding increases in water supply. Our projections also indicate increases in WSI in certain semi-arid and arid regions, attributed to CO<sub>2</sub>- and climate-induced expansions in vegetation cover and leaf area, reducing water availability in already water-limited areas. When averaged across IPCC climate regions and river basins, incorporating of all vegetation responses partially reduces projected WSI for most of the global population.

520 Modelling the complex interactions between the biosphere and hydrosphere under changing climate involves inherent limitations. The results presented here rely on assumptions and parameterisations in the JULES land surface model. Further research, particularly using improved representations of plant responses to elevated CO<sub>2</sub> and climate change, supported by observational data, is needed. Gathering large-scale empirical evidence on the strength of plant responses to CO<sub>2</sub> at large scales 525 will address modelling uncertainties and improve the reliability of future water scarcity projections for policymakers and water resource managers.

## **Appendices**

### **Appendix A**

#### **The four JULES simulations and calculations for the “isolated factors”**

		Vegetation structure (includes coverage, LAI and canopy height)		Calculations for isolated factor(s):
		Dynamic vegetation off (fixed at preindustrial)	Dynamic vegetation on	
<b>CO<sub>2</sub> levels in JULES affecting stomatal aperture</b>	<b>277 ppm</b> (fixed at preindustrial) <b>RCP 6.0</b>	S1. CLIM: STOM	S2. CLIM: STOM+VEG	<b>S2 - S1.</b> <b>CLIM: VEG</b>
<b>Calculations for isolated factor(s):</b>		S3. CLIM+CO <sub>2</sub> : STOM	S4. CLIM+CO <sub>2</sub> : STOM+VEG	<i>Not used</i>
		S3 - S1. <b>CO<sub>2</sub>: STOM</b>	S4 - S2. <b>CO<sub>2</sub>: STOM+VEG</b>	<b>S4 - S1.</b> <b>CO<sub>2</sub>: STOM &amp; CLIM+CO<sub>2</sub>: VEG</b>

530 **Table A1: The four JULES simulations driven by identical climate model output, and a combination of fixing plant CO<sub>2</sub> and structural vegetation responses.**

## Appendix B

### Stomatal Conductance Scheme used in JULES.

The version of JULES used in this study uses a coupled canopy conductance and photosynthesis model (Cox et al., 1998)

535 where stomatal conductance to water vapour  $g_s$  ( $\text{m s}^{-1}$ ) is based on:

$$g_s = -1.6A \frac{RT^*}{c_i - c_a} \quad (1)$$

where  $A$  is the net photosynthetic rate ( $\text{mol CO}_2 \text{ m}^{-2} \text{ s}^{-1}$ ),  $R$  is the universal gas constant ( $\text{J K}^{-1} \text{ mol}^{-1}$ ),  $T^*$  is the leaf surface temperature (K),  $c_i$  the internal CO<sub>2</sub> partial pressure (Pa),  $c_a$  the leaf surface CO<sub>2</sub> partial pressure (Pa) and factor of 1.6 accounting for molecular diffusivity differences between water and CO<sub>2</sub>. Vapour deficit at the leaf surface ( $D$ ,  $\text{kg kg}^{-1}$ )

540 affects stomatal conductance through the gradient between  $c_a$  and  $c_i$  is based on the equation by Jacobs (1994):

$$\frac{c_i - \Gamma^*}{c_a - \Gamma^*} = f_0 \left( 1 - \frac{D}{D_{crit}} \right) \quad (2)$$

where  $\Gamma^*$  is the photorespiration compensation point (Pa) and  $D_{crit}$  and  $f_0$  are PFT-specific calibration parameters, which are directly related to the parameters from the Leuning (1995) model (for details see Cox et al., 1998). Potential non-stressed leaf level photosynthesis is calculated in JULES using the C3 and C4 photosynthesis models of Collatz et al. (1991) and

545 Collatz et al. (1992) respectively.

The Jacobs formulation is a simplified version of the Leuning (1995) model, which in turn is based on the (Ball et al., 1987) model but depends on humidity deficit at the leaf surface instead of relative humidity.

## 550 **Runoff processes in JULES**

In this version of JULES, soil is divided into 4 layers, each with its own water content, which is determined by considering the inputs, such as precipitation, and outputs such as evapotranspiration and infiltration. The moisture content of each soil layer influences water movement, affecting how much percolates downward to deeper layers or moves horizontally as lateral flow. Additionally, in this version of JULES a TOPMODEL-type scheme is included, based on Clark and Gedney (2008) and  
555 Gedney and Cox (2003). This accounts for the influence of topography on soil moisture and runoff, enhancing JULES's ability to simulate the sub-grid spatial variability. Surface runoff is generated when precipitation exceeds the soil's infiltration capacity, when the soil becomes fully saturated, or when sub-grid scale inundation occurs. In TOPMODEL-based schemes, sub-surface runoff, or "baseflow", occurs with lateral flow below the water table, and its magnitude is influenced by soil moisture and soil type.

560

### **Code availability**

Python has been used to conduct our analysis. Code is available on GitHub at <https://github.com/jessica-stacey/water-scarcity-plants-jules>.

## 565 **Data availability**

Output from JULES simulations can be made available upon request. Water demand data is available from the ISIMIP database (e.g., [https://data.isimip.org/search/query/amanww/tree/ISIMIP2b/OutputData/water\\_global/h08/hadgem2-es/](https://data.isimip.org/search/query/amanww/tree/ISIMIP2b/OutputData/water_global/h08/hadgem2-es/)). Population data is also available from the ISIMIP database (<https://data.isimip.org/datasets/6eee7c61-4baa-4b1d-aa81-d854f217f07e/>).

## 570 **Author contributions**

JS: Conceptualisation, investigation, methodology, formal analysis, visualisation, writing draft.

RAB: Conceptualisation, methodology, supervision, writing (review and editing)

AH: Supervision, methodology, validation, writing (review and editing)

LM: Supervision, writing (review and editing)

575 NG: Writing (review and editing)

### **Competing interests**

The authors declare that they have no conflict of interest.

## 580 **Acknowledgements**

The authors would like to thank Dr Camilla Mathison and Dr Eleanor Burke for their dedicated effort in setting up the JULES ISIMIP2b suite and their guidance for getting it running. We are also thankful to Dr Chantelle Burton for her technical support to JS on the project. We would like to thank Dr Peter Greve for his support in providing early-stage data (ultimately not used

in this study), guidance on obtaining monthly water demand data and discussions on calculating the Water Scarcity Index.  
585 Finally, we would like to express our gratitude to the ISIMIP (Inter-Sectoral Impact Model Intercomparison Project) team for  
maintaining high-quality datasets and fostering collaboration across the scientific community which have greatly contributed  
to the advancement of climate impact research. Also, we acknowledge the use of OpenAI's ChatGPT to enhance the clarity  
and accessibility of text drafted by JS, and GitHub's Copilot to refine code developed by JS for data analysis and visualisation.  
All outputs were meticulously reviewed, verified, and edited by JS to ensure accuracy, relevance, and adherence to scientific  
590 standards.

### **Financial support**

JS, RAB, AH and NG were supported by the Met Office Hadley Centre Climate Programme funded by the UK Department of  
Science, Innovation and Technology (DSIT). JS, RAB and NG were additionally supported by the AmazonFACE programme  
595 funded by the UK Foreign, Commonwealth and Development Office (FCDO) and JS and AH were further supported by the  
Climate Science for Service Partnership (CSSP) Brazil project funded by DSIT. LM acknowledges funding by UK Natural  
Environment Research Council project NE/W004895/1.

### **References**

- 600 Ball, J. T., Woodrow, I. E., and Berry, J. A.: A Model Predicting Stomatal Conductance and its Contribution to the Control of  
Photosynthesis under Different Environmental Conditions, in: *Progress in Photosynthesis Research: Volume 4 Proceedings of  
the VIIth International Congress on Photosynthesis Providence, Rhode Island, USA, August 10–15, 1986*, edited by: Biggins,  
J., Springer Netherlands, Dordrecht, 221–224, [https://doi.org/10.1007/978-94-017-0519-6\\_48](https://doi.org/10.1007/978-94-017-0519-6_48), 1987.
- Battipaglia, G., Saurer, M., Cherubini, P., Calfapietra, C., Mccarthy, H. R., Norby, R. J., and Francesca Cotrufo, M.: Elevated  
605 CO<sub>2</sub> increases tree-level intrinsic water use efficiency: Insights from carbon and oxygen isotope analyses in tree rings across  
three forest FACE sites, *New Phytologist*, 197, 544–554, <https://doi.org/10.1111/nph.12044>, 2013.
- Best, M. J., Pryor, M., Clark, D. B., Rooney, G. G., Essery, R. L. H., Ménard, C. B., Edwards, J. M., Hendry, M. A., Porson,  
A., Gedney, N., Mercado, L. M., Sitch, S., Blyth, E., Boucher, O., Cox, P. M., Grimmond, C. S. B., and Harding, R. J.: The  
Joint UK Land Environment Simulator (JULES), model description-Part 1: Energy and water fluxes, *Geosci. Model Dev*, 4,  
610 677–699, <https://doi.org/10.5194/gmd-4-677-2011>, 2011.
- Betts, R. A., Cox, P. M., Lee, S. E., and Woodward, F. I.: Contrasting physiological and structural vegetation feedbacks in  
climate change simulations, *Nature*, 387, 796–799, <https://doi.org/10.1038/42924>, 1997.
- Betts, R. A., Boucher, O., Collins, M., Cox, P. M., Falloon, P. D., Gedney, N., Hemming, D. L., Huntingford, C., Jones, C. D.,  
Sexton, D. M. H., and Webb, M. J.: Projected increase in continental runoff due to plant responses to increasing carbon dioxide,  
615 *Nature*, 448, 1037–1041, <https://doi.org/10.1038/nature06045>, 2007.

- Caretta, M. A., Mukherji, A., Arfanuzzaman, M., Betts, R. A., Gelfan, A., Hirabayashi, Y., Lissner, T. K., Liu, J., Gunn, E. L., Morgan, R., Mwanga, S., Supratid, S., Pörtner, H.-O., Roberts, D. C., Tignor, M., Poloczanska, E. S., Mintenbeck, K., Alegría, A., Craig, M., Langsdorf, S., Löschke, S., Möller, V., Okem, A., and Rama, B.: 2022: Water., In: *Climate Change 2022: Impacts, Adaptation, and Vulnerability. Contribution of Working Group II to the Sixth Assessment Report of the Intergovernmental Panel on Climate Change*, 551–712, <https://doi.org/10.1017/9781009325844.006.552>, 2022.
- 620 Cao, L., Bala, G., Caldeira, K., Nemani, R., and Ban-Weiss, G.: Importance of carbon dioxide physiological forcing to future climate change, *Proceedings of the National Academy of Sciences of the United States of America*, 107, 9513–9518, <https://doi.org/10.1073/pnas.0913000107>, 2010.
- Clark, D. B. and Gedney, N.: Representing the effects of subgrid variability of soil moisture on runoff generation in a land surface model, *Journal of Geophysical Research: Atmospheres*, 113, <https://doi.org/10.1029/2007JD008940>, 2008.
- 625 Clark, D. B., Mercado, L. M., Sitch, S., Jones, C. D., Gedney, N., Best, M. J., Pryor, M., Rooney, G. G., Essery, R. L. H., Blyth, E., Boucher, O., Harding, R. J., Huntingford, C., and Cox, P. M.: The Joint UK Land Environment Simulator (JULES), model description – Part 2: Carbon fluxes and vegetation dynamics, *Geoscientific Model Development*, 4, 701–722, <https://doi.org/10.5194/gmd-4-701-2011>, 2011.
- 630 Collatz, G. J., Ball, J. T., Grivet, C., and Berry, J. A.: Physiological and environmental regulation of stomatal conductance, photosynthesis and transpiration: a model that includes a laminar boundary layer, *Agricultural and Forest Meteorology*, 54, 107–136, [https://doi.org/10.1016/0168-1923\(91\)90002-8](https://doi.org/10.1016/0168-1923(91)90002-8), 1991.
- Collatz, G., Ribas-Carbo, M., and Berry, J.: Coupled Photosynthesis-Stomatal Conductance Model for Leaves of C4 Plants, *Functional Plant Biology*, 19, 519–538, <https://doi.org/10.1071/PP9920519>, 1992.
- 635 Cowan, I. R.: Stomatal Behaviour and Environment, *Advances in Botanical Research*, 4, 117–228, [https://doi.org/10.1016/S0065-2296\(08\)60370-5](https://doi.org/10.1016/S0065-2296(08)60370-5), 1978.
- Cowling, S. A. and Field, C. B.: Environmental control of leaf area production: Implications for vegetation and land-surface modeling, *Global Biogeochemical Cycles*, 17, 7-1-7–14, <https://doi.org/10.1029/2002GB001915>, 2003.
- 640 Cox, P. M., Huntingford, C., and Harding, R. J.: A canopy conductance and photosynthesis model for use in a GCM land surface scheme, 213, 79–94, 1998.
- Cox, P. M.: Description of the TRIFFID dynamic global vegetation model, *Theoretical and Applied Climatology*, 16, 2001.
- Davie, J. C. S., Falloon, P. D., Kahana, R., Dankers, R., Betts, R., Portmann, F. T., Wisser, D., Clark, D. B., Ito, A., Masaki, Y., Nishina, K., Fekete, B., Tessler, Z., Wada, Y., Liu, X., Tang, Q., Hagemann, S., Stacke, T., Pavlick, R., Schaphoff, S., Gosling, S. N., Franssen, W., and Arnell, N.: Comparing projections of future changes in runoff from hydrological and biome models in ISI-MIP, *Earth System Dynamics*, 4, 359–374, <https://doi.org/10.5194/esd-4-359-2013>, 2013.
- 645 De Kauwe, M. G., Medlyn, B. E., Zaehle, S., Walker, A. P., Dietze, M. C., Hickler, T., Jain, A. K., Luo, Y., Parton, W. J., Prentice, I. C., Smith, B., Thornton, P. E., Wang, S., Wang, Y.-P., Wårlind, D., Weng, E., Crous, K. Y., Ellsworth, D. S., Hanson, P. J., Seok Kim, H.-, Warren, J. M., Oren, R., and Norby, R. J.: Forest water use and water use efficiency at elevated :

- a model-data intercomparison at two contrasting temperate forest FACE sites, *Global Change Biology*, 19, 1759–1779, <https://doi.org/10.1111/gcb.12164>, 2013.
- 650 Dolan, F., Lamontagne, J., Link, R., Hejazi, M., Reed, P., and Edmonds, J.: Evaluating the economic impact of water scarcity in a changing world, *Nature Communications*, 12, 1–10, <https://doi.org/10.1038/s41467-021-22194-0>, 2021.
- Falkenmark, M., Lundqvist, J., and Widstrand, C.: Macro-scale water scarcity requires micro-scale approaches. Aspects of vulnerability in semi-arid development., *Natural resources forum*, 13, 258–267, <https://doi.org/10.1111/j.1477-8947.1989.tb00348.x>, 1989.
- 655 Falloon, P., Betts, R., and Bunton, C.: A new global river routing scheme in the Unified Model, Hadley Centre Technical Note 72, Met Office Hadley Centre. 2007.
- Field, C. B., Jackson, R. B., and Mooney, H. A.: Stomatal responses to increased CO<sub>2</sub>: implications from the plant to the global scale, *Plant, Cell & Environment*, 18, 1214–1225, <https://doi.org/10.1111/j.1365-3040.1995.tb00630.x>, 1995.
- 660 Fisher, R. A. and Koven, C. D.: Perspectives on the Future of Land Surface Models and the Challenges of Representing Complex Terrestrial Systems, *Journal of Advances in Modeling Earth Systems*, 12, e2018MS001453, <https://doi.org/10.1029/2018MS001453>, 2020.
- Fowler, M. D., Kooperman, G. J., Randerson, J. T., and Pritchard, M. S.: The effect of plant physiological responses to rising CO<sub>2</sub> on global streamflow, *Nature Climate Change*, 9, 873–879, <https://doi.org/10.1038/s41558-019-0602-x>, 2019.
- 665 Gedney, N. and Cox, P. M.: The Sensitivity of Global Climate Model Simulations to the Representation of Soil Moisture Heterogeneity, 2003.
- Gedney, N., Cox, P. M., Betts, R. A., Boucher, O., Huntingford, C., and Stott, P. A.: Detection of a direct carbon dioxide effect in continental river runoff records, *Nature*, 439, 835–838, <https://doi.org/10.1038/nature04504>, 2006.
- Gedney, N., Huntingford, C., Weedon, G. P., Bellouin, N., Boucher, O., and Cox, P. M.: Detection of solar dimming and brightening effects on Northern Hemisphere river flow, *Nature Geosci*, 7, 796–800, <https://doi.org/10.1038/ngeo2263>, 2014.
- 670 Gosling, S. N. and Arnell, N. W.: A global assessment of the impact of climate change on water scarcity, *Climatic Change*, 134, 371–385, <https://doi.org/10.1007/s10584-013-0853-x>, 2016.
- Gosling, S. N., Müller Schmied, H., Burek, P., Chang, J., Ciais, P., Döll, P., Eisner, S., Fink, G., Flörke, M., Franssen, W., Grillakis, M., Hagemann, S., Hanasaki, N., Koutroulis, A., Leng, G., Liu, X., Masaki, Y., Mathison, C., Mishra, V., Ostberg, S., Portmann, F., Qi, W., Sahu, R.-K., Satoh, Y., Schewe, J., Seneviratne, S., Shah, H. L., Stacke, T., Tao, F., Telteu, C., Thiery, W., Trautmann, T., Tsanis, I., Wanders, N., Zhai, R., Büchner, M., Schewe, J., and Zhao, F.: ISIMIP2b Simulation Data from the Global Water Sector, <https://doi.org/10.48364/ISIMIP.626689>, 2023.
- 675 Greve, P., Kahil, T., Mochizuki, J., Schinko, T., Satoh, Y., Burek, P., Fischer, G., Tramberend, S., Burtscher, R., Langan, S., and Wada, Y.: Global assessment of water challenges under uncertainty in water scarcity projections, *Nature Sustainability*, 1, 486–494, <https://doi.org/10.1038/s41893-018-0134-9>, 2018.
- 680 Haddeland, I., Heinke, J., Biemans, H., Eisner, S., Flörke, M., Hanasaki, N., Konzmann, M., Ludwig, F., Masaki, Y., Schewe, J., Stacke, T., Tessler, Z. D., Wada, Y., and Wisser, D.: Global water resources affected by human interventions and climate

- change, *Proceedings of the National Academy of Sciences of the United States of America*, 111, 3251–3256, <https://doi.org/10.1073/pnas.1222475110>, 2014.
- 685 Hanasaki, N., Kanae, S., Oki, T., Masuda, K., Motoya, K., Shirakawa, N., Shen, Y., and Tanaka, K.: An integrated model for the assessment of global water resources - Part 1: Model description and input meteorological forcing, *Hydrology and Earth System Sciences*, 12, 1007–1025, <https://doi.org/10.5194/hess-12-1007-2008>, 2008a.
- Hanasaki, N., Kanae, S., Oki, T., Masuda, K., Motoya, K., Shirakawa, N., Shen, Y., and Tanaka, K.: An integrated model for the assessment of global water resources – Part 2: Applications and assessments, *Hydrology and Earth System Sciences*, 12, 690 1027–1037, <https://doi.org/10.5194/hess-12-1027-2008>, 2008b.
- Hanasaki, N., Yoshikawa, S., Pokhrel, Y., and Kanae, S.: A global hydrological simulation to specify the sources of water used by humans, *Hydrology and Earth System Sciences*, 22, 789–817, <https://doi.org/10.5194/hess-22-789-2018>, 2018.
- Harper, A. B., Cox, P. M., Friedlingstein, P., Wiltshire, A. J., Jones, C. D., Sitch, S., Mercado, L. M., Groenendijk, M., Robertson, E., Kattge, J., Bönisch, G., Atkin, O. K., Bahn, M., Cornelissen, J., Niinemets, Ü., Onipchenko, V., Peñuelas, J., 695 Poorter, L., Reich, P. B., Soudzilovskaia, N. A., and Bodegom, P. van: Improved representation of plant functional types and physiology in the Joint UK Land Environment Simulator (JULES v4.2) using plant trait information, *Geoscientific Model Development*, 9, 2415–2440, <https://doi.org/10.5194/gmd-9-2415-2016>, 2016.
- Iturbide, M., Gutiérrez, J. M., Alves, L. M., Bedia, J., Cerezo-Mota, R., Gimeno, E., Cofiño, A. S., Di Luca, A., Faria, S. H., Gorodetskaya, I. V., Hauser, M., Herrera, S., Hennessy, K., Hewitt, H. T., Jones, R. G., Krakovska, S., Manzanar, R., 700 Martínez-Castro, D., Narisma, G. T., Nurhati, I. S., Pinto, I., Seneviratne, S. I., van den Hurk, B., and Vera, C. S.: An update of IPCC climate reference regions for subcontinental analysis of climate model data: definition and aggregated datasets, *Earth System Science Data*, 12, 2959–2970, <https://doi.org/10.5194/essd-12-2959-2020>, 2020.
- Jacobs, C. M. J.: Direct Impact of Atmospheric CO<sub>2</sub> Enrichment on Regional Transpiration, Wageningen Agricultural University, Ph.D. Thesis, 1994.
- 705 Jones, C. D., Hughes, J. K., Bellouin, N., Hardiman, S. C., Jones, G. S., Knight, J., Liddicoat, S., O’Connor, F. M., Andres, R. J., Bell, C., Boo, K. O., Bozzo, A., Butchart, N., Cadule, P., Corbin, K. D., Doutriaux-Boucher, M., Friedlingstein, P., Gornall, J., Gray, L., Halloran, P. R., Hurtt, G., Ingram, W. J., Lamarque, J. F., Law, R. M., Meinshausen, M., Osprey, S., Palin, E. J., Parsons Chini, L., Raddatz, T., Sanderson, M. G., Sellar, A. A., Schurer, A., Valdes, P., Wood, N., Woodward, S., Yoshioka, M., and Zerroukat, M.: The HadGEM2-ES implementation of CMIP5 centennial simulations, *Geoscientific Model* 710 *Development*, 4, 543–570, <https://doi.org/10.5194/gmd-4-543-2011>, 2011.
- Kooperman, G. J., Fowler, M. D., Hoffman, F. M., Koven, C. D., Lindsay, K., Pritchard, M. S., Swann, A. L. S., and Randerson, J. T.: Plant Physiological Responses to Rising CO<sub>2</sub> Modify Simulated Daily Runoff Intensity With Implications for Global-Scale Flood Risk Assessment, *Geophysical Research Letters*, 45, 12,457-12,466, <https://doi.org/10.1029/2018GL079901>, 2018.
- 715 Lange, S.: Trend-preserving bias adjustment and statistical downscaling with ISIMIP3BASD (v1.0), *Geoscientific Model Development*, 12, 3055–3070, <https://doi.org/10.5194/gmd-12-3055-2019>, 2019.

- Lehner, B. and Grill, G.: Global river hydrography and network routing: baseline data and new approaches to study the world's large river systems, *Hydrological Processes*, 27, 2171–2186, <https://doi.org/10.1002/hyp.9740>, 2013.
- Lemordant, L., Gentine, P., Swann, A. S., Cook, B. I., and Scheff, J.: Critical impact of vegetation physiology on the continental hydrologic cycle in response to increasing CO<sub>2</sub>, *Proceedings of the National Academy of Sciences of the United States of America*, 115, 4093–4098, <https://doi.org/10.1073/pnas.1720712115>, 2018.
- Leuning, R.: A critical appraisal of a combined stomatal-photosynthesis model for C<sub>3</sub> plants, *Plant, Cell & Environment*, 18, 339–355, <https://doi.org/10.1111/j.1365-3040.1995.tb00370.x>, 1995.
- Mankin, J. S., Seager, R., Smerdon, J. E., Cook, B. I., and Williams, A. P.: Mid-latitude freshwater availability reduced by projected vegetation responses to climate change, *Nature Geoscience*, 12, 983–988, <https://doi.org/10.1038/s41561-019-0480-x>, 2019.
- Mathison, C., Burke, E., Hartley, A. J., Kelley, D. I., Burton, C., Robertson, E., Gedney, N., Williams, K., Wiltshire, A., Ellis, R. J., Sellar, A. A., and Jones, C. D.: Description and evaluation of the JULES-ES set-up for ISIMIP2b, *Geoscientific Model Development*, 16, 4249–4264, <https://doi.org/10.5194/gmd-16-4249-2023>, 2023.
- Norby, R. J. and Zak, D. R.: Ecological lessons from free air carbon enhancement (FACE) experiments, *Annual Review of Ecology, Evolution, and Systematics*, 42, <https://doi.org/10.1146/annurev-ecolsys-102209-144647>, 2011.
- Parnesan, C., Morecroft, M. D., Trisurat, Y., Adrian, R., Anshari, G. Z., Arneth, A., Gao, Q., Gonzalez, P., Harris, R., Price, J., Stevens, N., and Talukdar, G. H.: Terrestrial and freshwater ecosystems and their services, in: *Climate Change 2022: Impacts, Adaptation and Vulnerability, Contribution of Working Group II to the Sixth Assessment Report of the Intergovernmental Panel on Climate Change*, edited by: Pörtner, H.-O., Roberts, D. C., Tignor, M., Poloczanska, E. S., Mintenbeck, K., Alegría, A., Craig, M., Langsdorf, S., Lösschke, S., Möller, V., Okem, A., and Rama, B., Cambridge University Press, Cambridge, UK and New York, NY, USA, 197–377, <https://doi.org/10.1017/9781009325844.004>, 2022.
- Piao, S., Friedlingstein, P., Ciais, P., De Noblet-Ducoudré, N., Labat, D., and Zaehle, S.: Changes in climate and land use have a larger direct impact than rising CO<sub>2</sub> on global river runoff trends, *Proceedings of the National Academy of Sciences of the United States of America*, 104, 15242–15247, <https://doi.org/10.1073/pnas.0707213104>, 2007.
- Piontek, F. and Geiger, T.: ISIMIP2b secondary population input data (1.0), <https://doi.org/10.48364/ISIMIP.432399>, 2017.
- Raskin, P. and Gleick, P. H.: *Water Futures: Assessment of Long-range Patterns and Problems*, Stockholm Environment Institute, Stockholm, 1997.
- Riahi, K., van Vuuren, D. P., Kriegler, E., Edmonds, J., O'Neill, B. C., Fujimori, S., Bauer, N., Calvin, K., Dellink, R., Fricko, O., Lutz, W., Popp, A., Cuaresma, J. C., KC, S., Leimbach, M., Jiang, L., Kram, T., Rao, S., Emmerling, J., Ebi, K., Hasegawa, T., Havlik, P., Humpenöder, F., Da Silva, L. A., Smith, S., Stehfest, E., Bosetti, V., Eom, J., Gernaat, D., Masui, T., Rogelj, J., Strefler, J., Drouet, L., Krey, V., Luderer, G., Harmsen, M., Takahashi, K., Baumstark, L., Doelman, J. C., Kainuma, M., Klimont, Z., Marangoni, G., Lotze-Campen, H., Obersteiner, M., Tabeau, A., and Tavoni, M.: The Shared Socioeconomic Pathways and their energy, land use, and greenhouse gas emissions implications: An overview, *Global Environmental Change*, 42, 153–168, <https://doi.org/10.1016/j.gloenvcha.2016.05.009>, 2017.

- Ripple, W. J., Wolf, C., Newsome, T. M., Galetti, M., Alamgir, M., Crist, E., Mahmoud, M. I., Laurance, W. F., and 15,364 scientist signatories from 184 countries: World Scientists' Warning to Humanity: A Second Notice, *BioScience*, 67, 1026–1028, <https://doi.org/10.1093/biosci/bix125>, 2017.
- Schewe, J., Heinke, J., Gerten, D., Haddeland, I., Arnell, N. W., Clark, D. B., Dankers, R., Eisner, S., Fekete, B. M., Colón-González, F. J., Gosling, S. N., Kim, H., Liu, X., Masaki, Y., Portmann, F. T., Satoh, Y., Stacke, T., Tang, Q., Wada, Y., Wissler, D., Albrecht, T., Frieler, K., Piontek, F., Warszawski, L., and Kabat, P.: Multimodel assessment of water scarcity under climate change, *Proceedings of the National Academy of Sciences of the United States of America*, 111, 3245–3250, <https://doi.org/10.1073/pnas.1222460110>, 2013.
- Schneider, U., Finger, P., Meyer-Christoffer, A., Rustemeier, E., Ziese, M., and Becker, A.: Evaluating the hydrological cycle over land using the newly-corrected precipitation climatology from the Global Precipitation Climatology Centre (GPCP), *Atmosphere*, 8, <https://doi.org/10.3390/atmos8030052>, 2017.
- Sellar, A. A., Jones, C. G., Mulcahy, J. P., Tang, Y., Yool, A., Wiltshire, A., O'Connor, F. M., Stringer, M., Hill, R., Palmieri, J., Woodward, S., de Mora, L., Kuhlbrodt, T., Rumbold, S. T., Kelley, D. I., Ellis, R., Johnson, C. E., Walton, J., Abraham, N. L., Andrews, M. B., Andrews, T., Archibald, A. T., Berthou, S., Burke, E., Blockley, E., Carslaw, K., Dalvi, M., Edwards, J., Folberth, G. A., Gedney, N., Griffiths, P. T., Harper, A. B., Hendry, M. A., Hewitt, A. J., Johnson, B., Jones, A., Jones, C. D., Keeble, J., Liddicoat, S., Morgenstern, O., Parker, R. J., Predoi, V., Robertson, E., Siahahaan, A., Smith, R. S., Swaminathan, R., Woodhouse, M. T., Zeng, G., and Zerroukat, M.: UKESM1: Description and Evaluation of the U.K. Earth System Model, *Journal of Advances in Modeling Earth Systems*, 11, 4513–4558, <https://doi.org/10.1029/2019MS001739>, 2019.
- Seneviratne, S. I., Zhang, X., Adnan, M., Badi, W., Dereczynski, C., Luca, A. D., Ghosh, S., Iskandar, I., Kossin, J., Lewis, S., Otto, F., Pinto, I., Satoh, M., Vicente-Serrano, S. M., Wehner, M., Zhou, B. and Allan, R.: Weather and climate extreme events in a changing climate, *Climate Change 2021: The Physical Science Basis: Working Group I contribution to the Sixth Assessment Report of the Intergovernmental Panel on Climate Change*. Cambridge University Press, 1513–1766, <https://doi.org/10.1017/9781009157896.013>, 2021.
- Sitch, S., Huntingford, C., Gedney, N., Levy, P. E., Lomas, M., Piao, S. L., Betts, R., Ciais, P., Cox, P., Friedlingstein, P., Jones, C. D., Prentice, I. C., and Woodward, F. I.: Evaluation of the terrestrial carbon cycle, future plant geography and climate-carbon cycle feedbacks using five Dynamic Global Vegetation Models (DGVMs), *Global Change Biology*, 14, 2015–2039, <https://doi.org/10.1111/j.1365-2486.2008.01626.x>, 2008.
- Sitch, S., O'Sullivan, M., Robertson, E., Friedlingstein, P., Albergel, C., Anthoni, P., Arneeth, A., Arora, V. K., Bastos, A., Bastrikov, V., Bellouin, N., Canadell, J. G., Chini, L., Ciais, P., Falk, S., Harris, I., Hurtt, G., Ito, A., Jain, A. K., Jones, M. W., Joos, F., Kato, E., Kennedy, D., Klein Goldewijk, K., Kluzek, E., Knauer, J., Lawrence, P. J., Lombardozzi, D., Melton, J. R., Nabel, J. E. M. S., Pan, N., Peylin, P., Pongratz, J., Poulter, B., Rosan, T. M., Sun, Q., Tian, H., Walker, A. P., Weber, U., Yuan, W., Yue, X., and Zaehle, S.: Trends and Drivers of Terrestrial Sources and Sinks of Carbon Dioxide: An Overview of the TRENDY Project, *Global Biogeochemical Cycles*, 38, e2024GB008102, <https://doi.org/10.1029/2024GB008102>, 2024.

- Swann, A. L. S., Hoffman, F. M., Koven, C. D., and Randerson, J. T.: Plant responses to increasing CO<sub>2</sub> reduce estimates of climate impacts on drought severity, *Proceedings of the National Academy of Sciences of the United States of America*, 113, 10019–10024, <https://doi.org/10.1073/pnas.1604581113>, 2016.
- Ukkola, A. M., Prentice, I. C., Keenan, T. F., Van Dijk, A. I. J. M., Viney, N. R., Myneni, R. B., and Bi, J.: Reduced streamflow in water-stressed climates consistent with CO<sub>2</sub> effects on vegetation, <https://doi.org/10.1038/NCLIMATE2831>, 2016.
- Walker, A. P., Hanson, P. J., De Kauwe, M. G., Medlyn, B. E., Zaehle, S., Asao, S., Dietze, M., Hickler, T., Huntingford, C., Iversen, C. M., Jain, A., Lomas, M., Luo, Y., McCarthy, H., Parton, W. J., Prentice, I. C., Thornton, P. E., Wang, S., Wang, Y.-P., Warlind, D., Weng, E., Warren, J. M., Woodward, F. I., Oren, R., and Norby, R. J.: Comprehensive ecosystem model-data synthesis using multiple data sets at two temperate forest free-air CO<sub>2</sub> enrichment experiments: Model performance at ambient CO<sub>2</sub> concentration, *Journal of Geophysical Research: Biogeosciences*, 119, 937–964, <https://doi.org/10.1002/2013JG002553>, 2014.
- Wang, T. and Sun, F.: Socioeconomic exposure to drought under climate warming and globalization: The importance of vegetation-CO<sub>2</sub> feedback, *International Journal of Climatology*, n/a, <https://doi.org/10.1002/joc.8174>, 2023.
- Wei, H., Zhang, Y., Huang, Q., Chiew, F. H. S., Luan, J., Xia, J., and Liu, C.: Direct vegetation response to recent CO<sub>2</sub> rise shows limited effect on global streamflow, *Nat Commun*, 15, 9423, <https://doi.org/10.1038/s41467-024-53879-x>, 2024.
- Wei, Z., Yoshimura, K., Wang, L., Miralles, D. G., Jasechko, S., and Lee, X.: Revisiting the contribution of transpiration to global terrestrial evapotranspiration, *Geophysical Research Letters*, 44, 2792–2801, <https://doi.org/10.1002/2016GL072235>, 2017.
- Wigley, T. M. L. and Jones, P. D.: Influences of precipitation changes and direct CO<sub>2</sub> effects on streamflow, *Nature*, 314, 149–152, <https://doi.org/10.1038/314149a0>, 1985.
- Wiltshire, A., Gornall, J., Booth, B., Dennis, E., Falloon, P., Kay, G., McNeall, D., McSweeney, C., and Betts, R.: The importance of population, climate change and CO<sub>2</sub> plant physiological forcing in determining future global water stress, *Global Environmental Change*, 23, 1083–1097, <https://doi.org/10.1016/j.gloenvcha.2013.06.005>, 2013a.
- Wiltshire, A. J., Kay, G., Gornall, J. L., and Betts, R. A.: The impact of climate, CO<sub>2</sub> and population on regional food and water resources in the 2050s, *Sustainability (Switzerland)*, 5, 2129–2151, <https://doi.org/10.3390/su5052129>, 2013b.
- Xu, H., Wang, X., and Yang, T.: Trend shifts in satellite-derived vegetation growth in Central Eurasia, 1982–2013, *Science of The Total Environment*, 579, 1658–1674, <https://doi.org/10.1016/j.scitotenv.2016.11.182>, 2017.
- Yang, H., Huntingford, C., Wiltshire, A., Sitch, S., and Mercado, L.: Compensatory climate effects link trends in global runoff to rising atmospheric CO<sub>2</sub> concentration, *Environmental Research Letters*, 14, 124075, <https://doi.org/10.1088/1748-9326/ab5c6f>, 2019.
- Yu, T., Sun, R., Xiao, Z., Zhang, Q., Liu, G., Cui, T., and Wang, J.: Estimation of Global Vegetation Productivity from Global LAnd Surface Satellite Data, *Remote Sensing*, 10, 327, <https://doi.org/10.3390/rs10020327>, 2018.
- Zhu, Z., Piao, S., Myneni, R. B., Huang, M., Zeng, Z., Canadell, J. G., Ciais, P., Sitch, S., Friedlingstein, P., Arneeth, A., Cao, C., Cheng, L., Kato, E., Koven, C., Li, Y., Lian, X., Liu, Y., Liu, R., Mao, J., Pan, Y., Peng, S., Peuelas, J., Poulter, B., Pugh,

T. A. M., Stocker, B. D., Viovy, N., Wang, X., Wang, Y., Xiao, Z., Yang, H., Zaehle, S., and Zeng, N.: Greening of the Earth and its drivers, *Nature Climate Change*, 6, 791–795, <https://doi.org/10.1038/nclimate3004>, 2016.